Schweizerische Eidgenossenschaft
Confédération suisse
Confederazione Svizzera
Confederaziun svizra

Eidgenössisches Departement des Innern EDI
Bundesamt für Meteorologie und Klimatologie MeteoSchweiz

Arbeitsbericht MeteoSchweiz Nr. 219

Extreme Value Analysis of Wind Speed Observations over Switzerland

P. Ceppi, P.M. Della-Marta, C. Appenzeller

Arbeitsbericht MeteoSchweiz Nr. 219

Extreme Value Analysis of Wind Speed Observations over Switzerland

P. Ceppi, P.M. Della-Marta, C. Appenzeller

Bitte zitieren Sie diesen Arbeitsbericht folgendermassen
Ceppi, P., Della-Marta, P.M., Appenzeller, C.: 2008, Extreme Value Analysis of Wind Speed Observations over Switzerland, *Arbeitsberichte der MeteoSchweiz*, **219**, 48pp.

Herausgeber
Bundesamt für Meteorologie und Klimatologie, MeteoSchweiz, © 2008

MeteoSchweiz
Krähbühlstrasse 58
CH-8044 Zürich
T +41 44 256 91 11
www.meteoschweiz.ch

Weitere Standorte
CH-8058 Zürich-Flughafen
CH-6605 Locarno Monti
CH-1211 Genève 2
CH-1530 Payerne

Abstract

Accurate assessment of the magnitude and frequency of extreme wind speed is of fundamental importance for many safety, engineering and financial applications. However, extreme winds are coupled with local, small-scale phenomena, so that their spatial distribution is very inhomogeneous. So far, only limited information on extreme wind statistics was available for Swiss measuring stations.

We estimate the return period (frequency) of extreme wind speeds at 55 measuring stations over Switzerland. We utilise daily maximum 1-second wind gust measurements for the period 1981 - 2007 in order to create a local-scale extreme wind climatology. These measurements are checked for quality to ensure that they are suitable for an extreme value analysis, and their seasonal and long-term variability is examined.

In our analysis, we apply classical *peak over threshold* (POT) extreme value analysis techniques to the extreme wind data. Autocorrelation in the POT series is first eliminated by using a standard declustering technique; the series are then modelled using a *Generalised Pareto Distribution* (GPD) which is fitted using maximum likelihood estimation (MLE). We included estimates of the uncertainty in the return level and return period of extreme winds, which were calculated using likelihood profile methods.

Our results show that the data quality is generally good, with no obvious jumps or outliers; no long-term trends were visible. Generally, the choice of threshold and the declustering technique result in very good model fits. At some stations, however, the peaks deviate systematically from the model fit. Regional differences in wind climatologies, expected due to orography, are well reproduced. In particular, the exposure to westerly and Föhn winds seems to play a key role in the extreme wind distribution. However, the shape of the GPD model fits is quite homogeneous; they all have an upper bound, with one exception. The return periods of selected storms also feature large variability from one station to another; return periods for the storm Lothar range from <2 to >100 years, with most values on the Swiss Plateau lying above 10 years. This variability reflects the very complex behaviour of extreme winds at surface level.

Contents

List of Tables

List of Figures

Chapter 1

Introduction

1.1 Project background

Accurate knowledge of the frequency distribution of strong surface wind, in particular wind gusts, is of major relevance for many safety, engineering and financial applications. However, no accurate extreme wind statistics for Swiss measuring stations were available so far. This bachelor thesis builds upon a previous project at MeteoSwiss, which involved using reanalysis data to obtain continental and regional scale return period estimates of prominent wind storm events (Della-Marta et al., 2007). This work was based upon the ECMWF ERA40 model reanalysis, which may not reproduce regional or local features. Indeed, reanalysis wind speed data at the surface is a parametrised quantity, has biases in the wind speed magnitude and may not be representative of local wind speed given the coarse resolution of the reanalysis model. It is therefore not suitable for a detailed analysis of wind at local scales. To obtain accurate local scale wind frequency estimates it is necessary to use in-situ wind data.

Thus, this thesis considers station data only, i.e. daily maximum 1-second wind gusts from Swiss stations. Nevertheless, reliable climatologies based on in-situ wind observations are difficult to obtain as the observations are too coarse in space and/or short and inhomogeneous in time. Thus, one of the aims of our work is to assess the potential for creating an extreme wind climatology based on station measurements in Switzerland.

1.2 Practical applications

Our work provides detailed information about the magnitude and frequency of severe wind storms over Switzerland, including uncertainty estimates; this leads to a better understanding of the impacts of severe winds, both in the past and the future. This study also points out regional differences in the extreme wind climatologies. Knowledge of such information is essential for many safety, engineering or financial applications; in particular, it is highly relevant for insurance companies.

Another possible application for this work is in the field of climatological analyses, as it makes it possible to estimate the "extremeness" of a particular storm. As an example, it allows to calculate the return period of the storm "Lothar" for all the considered Swiss stations.

The remainder of the thesis is divided into four chapters. First we explain the data and methods used to determine the return period of extreme wind events. In the following chapters we present the main results and then conclude with some discussion and recommendations for future research.

Chapter 2

Datasets and Data Quality

2.1 Datasets

The data we considered in our analysis consists in daily maximum wind gusts, i.e. there is one value per day. This data was measured at automated stations from the SwissMetNet network, which comprises 132 stations in Switzerland. We included lowland as well as mountain or valley stations.

The considered time period is 1981-2007. Daily maximum wind gust measurements are available since 1981 only, so we chose only the stations with complete measurement series. This ensures a sufficient length for the statistical analysis, since all of the analysed stations have an equal amount of data. Table 2.1 shows a list of the considered stations, and their spatial distribution is represented in figure 2.1.

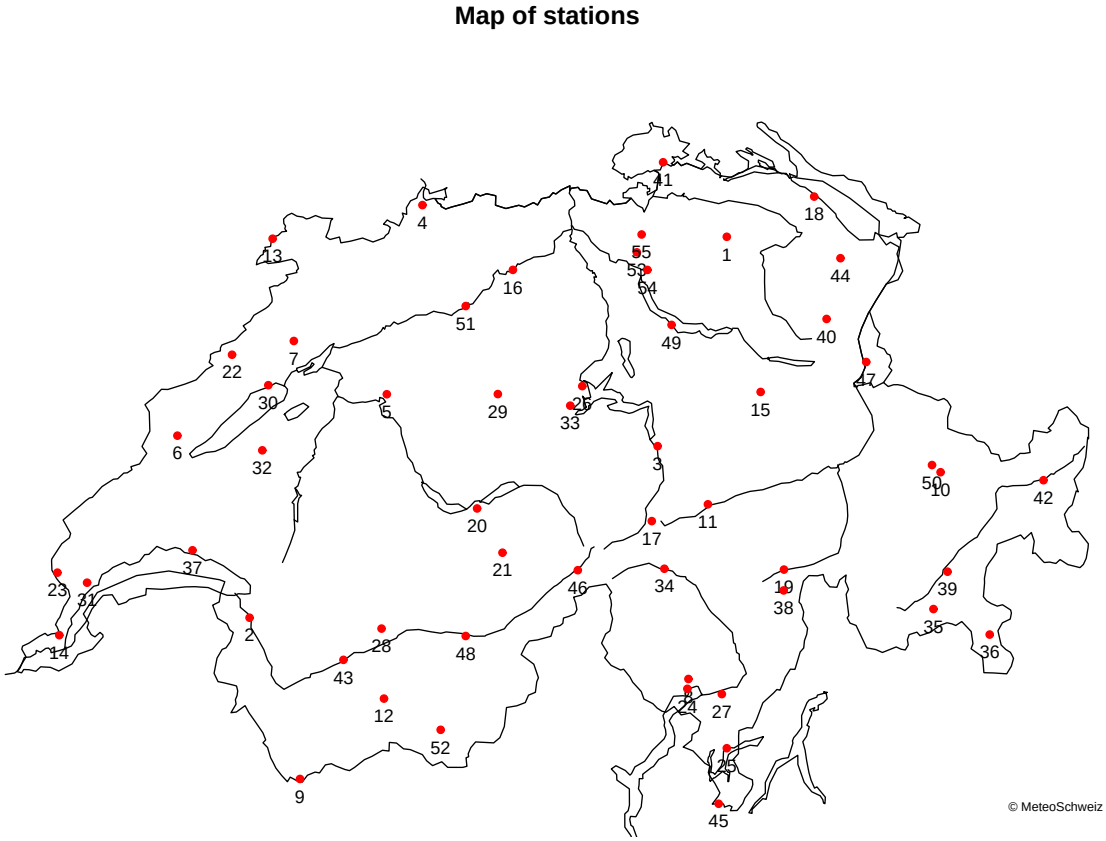

Figure 2.1: Spatial distribution of stations used in this study. The station numbers refer to the numbers in table 2.1.

	Station name	Height (m)		Station name	Height (m)
1	Aadorf / Tänikon	539	29	Napf	1404
2	Aigle	381	30	Neuchâtel	485
3	Altdorf	449	31	Nyon / Changins	455
4	Basel / Binningen	316	32	Payerne	490
5	Bern / Zollikofen	553	33	Pilatus	2106
6	Bullet / La Frétaz	1205	34	Piotta	1007
7	Chasseral	1599	35	Piz Corvatsch	3315
8	Cimetta	1672	36	Poschiavo / Robbia	1078
9	Col du Gd-St-Bernard	2472	37	Pully	456
10	Davos	1594	38	S. Bernardino	1639
11	Disentis / Sedrun	1197	39	Samedan	1709
12	Evolène / Villa	1825	40	Säntis	2502
13	Fahy	596	41	Schaffhausen	437
14	Genève-Cointrin	420	42	Scuol	1304
15	Glarus	517	43	Sion	482
16	Gösgen	380	44	St. Gallen	776
17	Gütsch ob Andermatt	2287	45	Stabio	353
18	Güttingen	440	46	Ulrichen	1345
19	Hinterrhein	1611	47	Vaduz	457
20	Interlaken	577	48	Visp	640
21	Jungfraujoch	3580	49	Wädenswil	463
22	La Chaux-de-Fonds	1018	50	Weissfluhjoch	2690
23	La Dôle	1670	51	Wynau	422
24	Locarno / Monti	367	52	Zermatt	1638
25	Lugano	273	53	Zürich / Affoltern	444
26	Luzern	454	54	Zürich / Fluntern	556
27	Magadino / Cadenazzo	203	55	Zürich / Kloten	436
28	Montana	1508			

Table 2.1: List of stations. Numbers in the first and fourth columns refer to the station numbers in figure 2.1.

2.2 Data Quality

Prior to the extreme value analysis, the data was roughly checked for quality. This step is important because the statistical analysis requires that the measurement series be homogeneous. In particular, there should be no non-climatic trends (e.g. due to changes in measurement methods or in measurement conditions), no inconsistent values (e.g. unrealistic wind peaks) and no long gaps.

It is known that wind measurements are very sensitive to local, small-scale effects which are difficult to predict. For this reason, it appears plausible that measuring conditions at a particular station may change over time: in particular, changes in land use (vegetation, buildings) next to a measurement station may have a considerable impact on the wind climatology. Of course, this would also affect the magnitude of peak wind gusts, and thus the frequency of extreme events, making the extreme value analysis inaccurate. In such a case, the measurement series could show a long-term trend, or a "jump", i.e. a sudden break in the series where the mean wind changes.

Our quality check was performed through a visual inspection of the time series. Three parameters were considered: daily maximum wind gusts (e.g. figure 2.2), as well as monthly and seasonal averages of the latter (not shown). These parameters were represented graphically

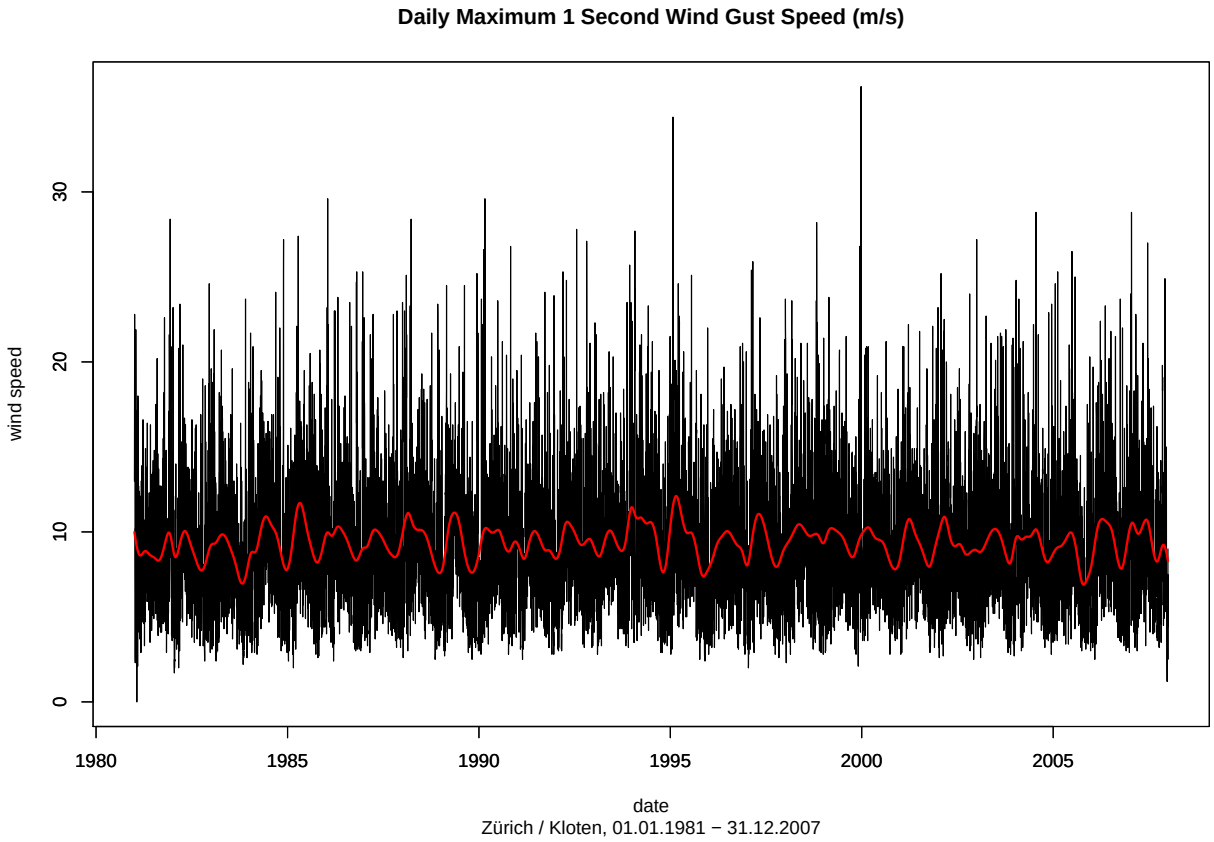

Figure 2.2: Daily maximum wind gusts 1981-2007 in Zürich / Kloten. The red curve is a cubic smoothing spline of the measurement series, for better visualisation of the long-term variability. This plot also gives an impression of the magnitude and frequency of extreme wind gusts. The highest visible peak (26.12.1999) corresponds to the storm Lothar.

as functions of time for each of the considered stations. The plots allowed us to identify some inconsistent values (e.g. peaks of 99.9 m/s), which were then removed manually. They also gave us a first impression of the distribution of extreme wind gusts, and in particular of their magnitude and frequency.

However, none of the graphs showed any obvious trends or gaps or jumps, which indicates that the homogeneity of the measurement series is good. As an example, on figure 2.2 we show the measurement series of Zürich / Kloten. A cubic smoothing spline (red curve) was fitted to the wind speed values for better visualisation of the seasonal and long-term variability; it shows that the wind gust values do not increase or decrease over time, i.e. there is no trend. There are also no obvious jumps or outliers. The results were similar for all other stations. The monthly and seasonal averages did not feature any significant long-term variations, either. Thus, no station had to be removed from the dataset because of inhomogeneity issues.

Chapter 3

Extreme Value Analysis

3.1 Definition

The purpose of extreme value analysis (EVA) is to find reliable estimates of the frequency of extreme events. In statistical terms, the frequency is usually expressed as a *return period* (RP) and the value which corresponds to that RP is called the *return level* (RL). (For some examples, see results in section 4.1.)

It is often the case that when quantifying extremes of any physical process there are limited observations of such a process. Usually, from an application point of view, we require information about extremes which have not been observed; this requires extrapolation of information from the observations at hand. In other words, EVA allows us to estimate RLs even for RPs larger than the period of observation. The analysis includes uncertainty calculations, with confidence intervals measuring the accuracy of parameter estimates.

EVA is based on the asymptotic behaviour of observed extremes; for a theoretical definition, see Fisher and Tippett (1928); Coles (2001). Palutikof et al. (1999) review common methods used to estimate the extreme value distribution of extreme wind speeds.

3.2 The Peak Over Threshold (POT) method

Note: parts of this section were adapted from Della-Marta et al. (2007), section 3.1.

The POT approach provides a model for independent exceedances above a large threshold. Assuming that exceedances are independent, identically distributed random variables, the distribution of exceedances asymptotes to a limit distibution, the *Generalised Pareto Distribution* (GPD). For more details, see Coles (2001), p. 76.

Thus, the GPD can be used to model exceedances above a given threshold. This distribution can be written in terms of a generic variable x as:

$$G(x) = 1 - \left[1 + \xi(\frac{x-u}{\sigma})\right]^{-\frac{1}{\xi}} \qquad (x > u,\, \xi \neq 0) \tag{3.1}$$

where u is the selected threshold.

The GPD function is a so-called *cumulative distribution function*, so it can be expressed in terms of probabilities. Let X be an independent and identically distributed random variable of the GPD function. Then equation 3.1 can be rewritten as follows:

$$\begin{aligned} &\Pr(X < x \mid x > u) = G(x) \\ &\Pr(X > x \mid x > u) = 1 - G(x) \\ &\Pr(X > x) = \Pr(x > u)\,[1 - G(x)] \end{aligned} \tag{3.2}$$

a) b)

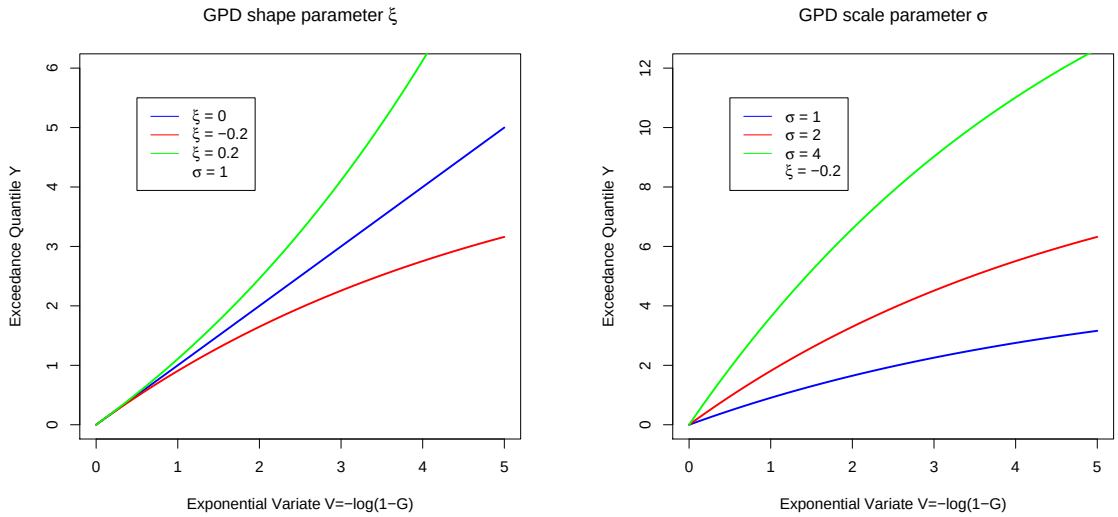

Figure 3.1: Influence of a) the shape parameter ξ and b) the scale parameter σ on the GPD curve.

$$\Pr(X > x) = \zeta_u \left[1 + \xi \left(\frac{x-u}{\sigma}\right)\right]^{-\frac{1}{\xi}} \tag{3.3}$$

where $\zeta_u = \Pr(X > u)$, i.e. ζ_u is the probability of the occurrence of an exceedance of a high threshold, u.

The GPD is characterised by two parameters, ξ the shape parameter and σ the scale parameter. The shape parameter determines tail behaviour: if $\xi > 0$ then the maximum of the GPD is unbounded, whereas if $\xi < 0$ then the tail has a finite extent. If $\xi = 0$, the GPD reduces to the exponential distribution and is also unbounded in the limit $\xi \to 0$. As for the scale parameter, it measures the scale or "amplitude" of the distribution. The effects of both parameters are displayed on figure 3.1.

In this study we are primarily interested in the the N-year return level (RL) x_N, which is exceeded once every N years. It can be expressed as

$$x_N = u + \frac{\sigma}{\xi}\left[(N n_y \zeta_u)^{\xi} - 1\right] \tag{3.4}$$

where n_y is the number of observations per year. (For a derivation of this formula, see Coles (2001).) Equation 3.4 suggests that in order to determine the N-year RL three parameters need to be fitted, ξ, σ and ζ_u. If we assume that these are rare events, ζ_u could be expected to follow a Poisson distribution. Here we deviate slightly from Coles (2001) who suggests ζ_u could be modelled by the binomial distribution. The Poisson distribution is characterised by the parameter λ, the mean number of threshold exceedances per unit time. We can estimate $\zeta_u \approx \lambda / n_y$ and reformulating equation 3.4 in terms of the λ (as also shown by Palutikof et al., 1999) we get:

$$x_N = u + \frac{\sigma}{\xi}\left[(\lambda N)^{\xi} - 1\right] \tag{3.5}$$

We estimated ξ and σ in equation 3.5 using maximum likelihood method (Martins and Stedinger, 2000; Coles, 2001; details not shown).

3.3 Declustering and threshold selection

As mentioned in section 3.2, the POT model requires that the exceedances be mutually independent. However, in the case of wind peaks this assumption may be violated because of serial correlation. Indeed, extreme winds over Europe are often associated with mesoscale and synoptic scale cyclones (Wernli et al., 2002). Typically these systems have a lifetime of around 72 hours or less. Since the time resolution of our data is as high as 24 hours, the wind gust peaks are expected to be somewhat dependent.

The most widely adopted method for dealing with this issue is *declustering*, which filters the dependent observations to obtain a set of threshold excesses that are approximately independent. This is done by defining an empirical rule to identify clusters of exceedances and identifying the cluster maxima; these maxima are called *declustered peaks* and are assumed to be independent. The declustered peaks are then fitted to the GPD.

Here we use a so-called *runs-declustering technique*. First, we set a threshold and we define clusters to be wherever there are consecutive exceedances of this threshold. We then set a run length (minimum separation) between each cluster; a cluster is terminated whenever the separation between two threshold exceedances is greater than the run length. In our analysis we chose a minimum separation of five days; this should ensure that the declustered peaks are independent from each other. Other common declustering methods are described in Coles (2001).

The threshold selection was performed using a number of different diagnostics. The latter are needed to ascertain that the threshold is high enough to be in the asymptotic limit of the distribution of exceedances. According to the postulates of the GPD, both the modified scale parameter $\sigma*$ (see Coles, 2001) and the shape parameter should be invariant with threshold within the asymptotic limit. Moreover, the mean of exceedances above a threshold u should be a linear function of u. The three plots in figure 3.2 show the threshold diagnostics for the Zürich / Fluntern station, following the methods described in Coles (2001). The threshold diagnostic plots show that for most stations, the 90% quantile is an appropriate threshold. This threshold was chosen as low as possible to enable as many peaks to be above the threshold and still satisfy the requirements of the GPD.

3.4 Uncertainty calculations

Several methods can be used to estimate confidence intervals. The method we use is *profile log-likelihood* as it seems to be the most suitable one for extreme wind statistics (Della-Marta et al., 2007). Compared to other uncertainty calculation methods, it has the advantage that it utilises more information from the sample, especially the information provided by the most extreme events. Using this method, it is also possible to obtain asymmetric uncertainty estimates, which, according to Coles (2001), are more precise and should be used in situations where it is necessary to obtain accurate confidence intervals.

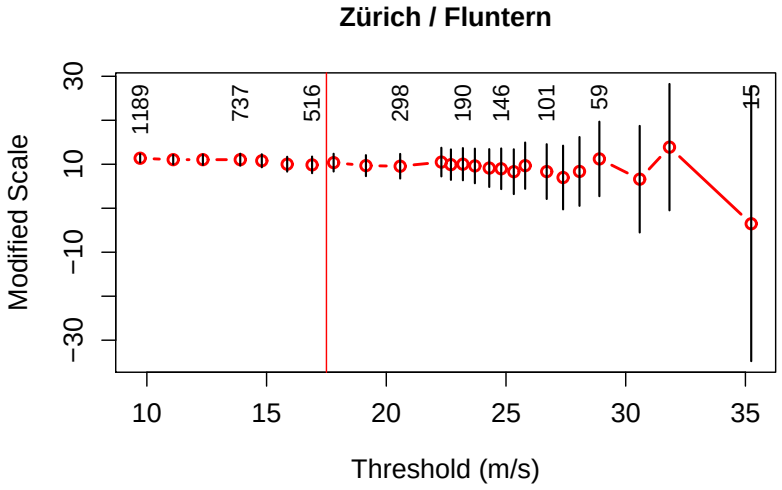

a)

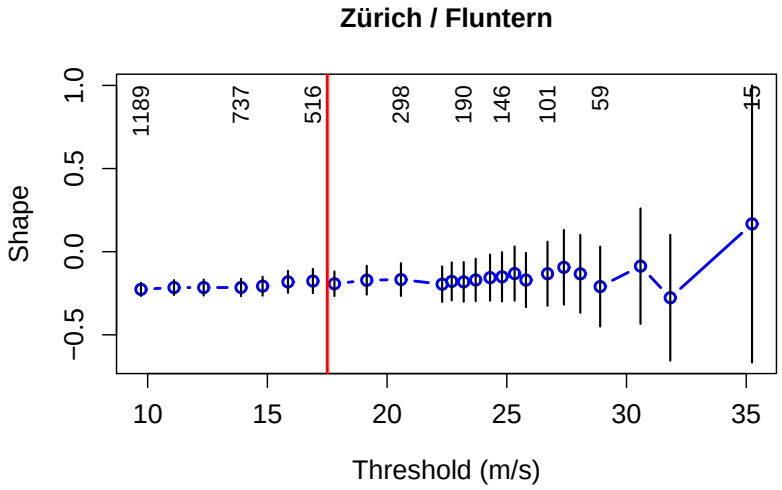

b)

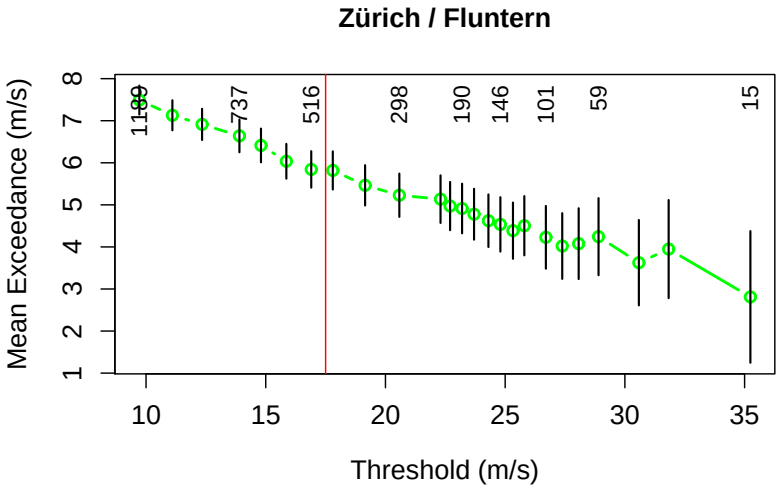

c)

Figure 3.2: a) Modified scale, $\sigma*$ (see Coles, 2001), b) shape, ξ, and c) mean exceedance parameter diagnostic plots for selecting the fixed threshold above which the declustered POT will be modelled using the GPD. The vertical black lines denote the 95% confidence intervals calculated using the parametric resampling technique detailed in section 3.4. The numbers aligned vertically in the top of the plot are the number of peaks above a given threshold. The vertical red line represents the selected threshold, corresponding to the 90% quantile.

Chapter 4

Results

4.1 Extreme wind distribution at Swiss stations

We applied the extreme value analysis methods described in chapter 3 to the declustered POT series of the 55 stations in our dataset. The results of the GPD fit are represented graphically with the return level (RL) as a function of the return period (RP); figures 4.1 and 4.2 show some examples. The complete extreme wind climatology for all stations is displayed in Appendix A on figures A.1 to A.9. The RL/RP plots represent the declustered wind peaks above the chosen threshold together with the GPD fit and the 95% confidence intervals. The confidence intervals describe the uncertainty associated with the parameter estimates. The declustered peaks of the POT series are also represented as black dots. Note that the x-coordinates of these peaks are determined basing only on an empirical estimation of the return period, and not using the fit information. We can see that the estimated RPs of the wind peaks feature a very wide range, from approximately 0.1 to >100 years.

One of the striking features of the RL/RP plots is that the shape parameter ξ of the GPD fit is almost always negative. This means that the extreme wind distributions have a finite upper bound (see section 3.2); they do not tend to infinity. In section 4.2 the spatial distribution of the GPD parameters is analysed in more detail.

The results show that in most cases the GPD fit of the time series is good; this is confirmed by the quantile-quantile plots (see figure 4.3 a) - d)). However, at some stations (about ten) the empirical values show systematic deviation from modelled values (figure 4.3 e) - f)). The deviations are particularly large at Ticino stations; as an example, we show the model fit for Locarno / Monti (figure 4.3 e)). Here a large part of the observed peaks are systematically below the model fit. Such systematic deviations also happen for different threshold values, so the selected threshold does not seem to be the cause of the problem. Nevertheless, we decided to keep the concerned stations in our analysis, since the deviation from the model does not appear critical at any of these stations.

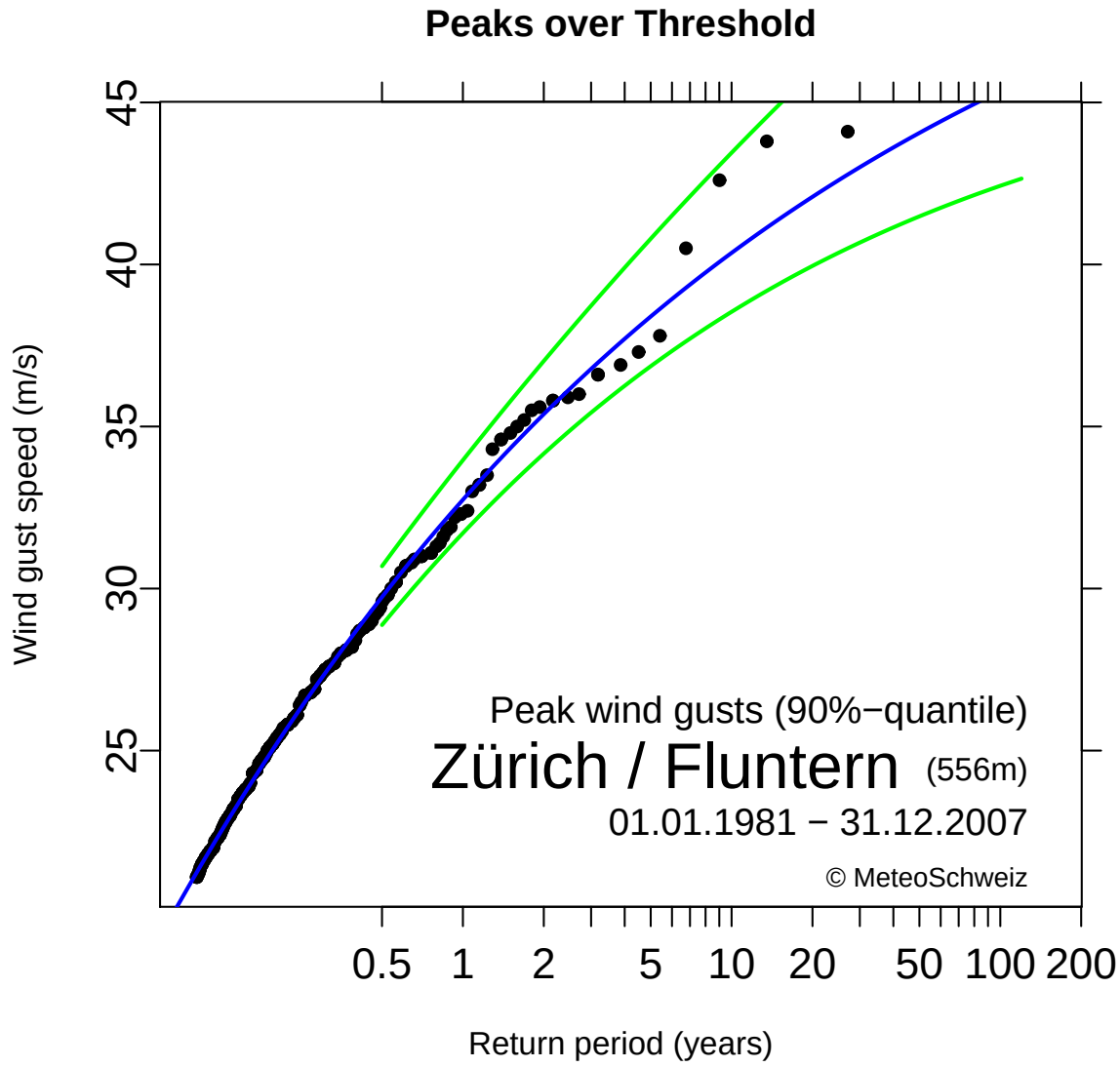

Figure 4.1: RL as a function of RP at Zürich / Fluntern station. The blue curve represents the GPD fit and the black dots are the declustered peaks of the POT series. The green curves show the upper and lower bounds of the 95% confidence interval. The dates of the four most extreme events are shown. Note the log scale on the horizontal axis.

a)

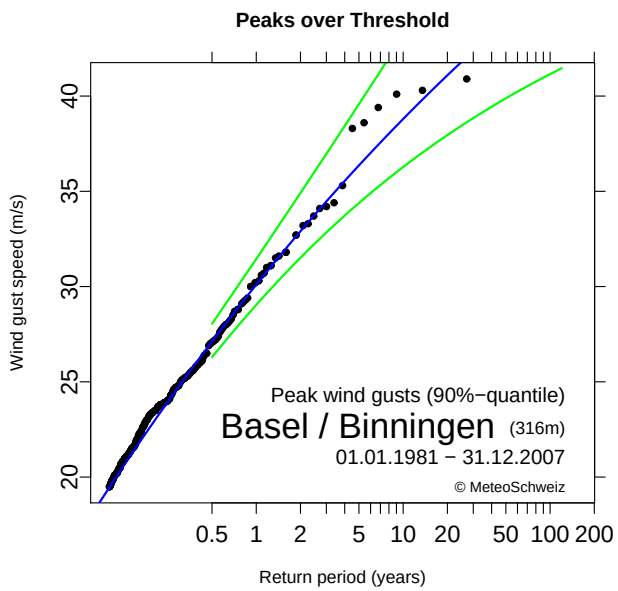

b)

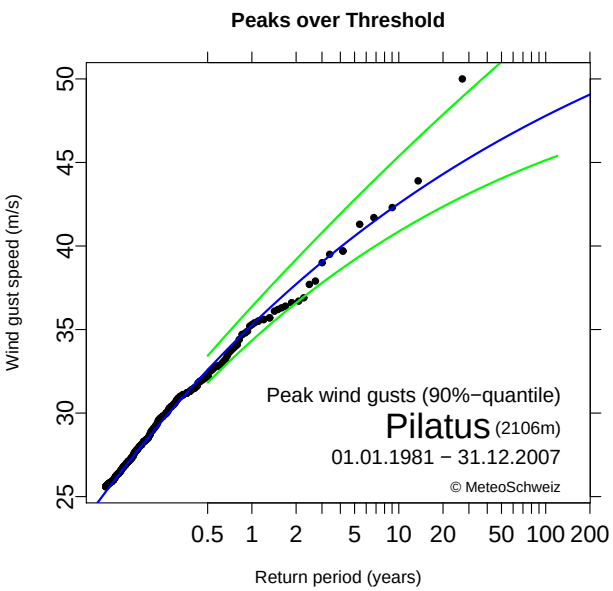

c)

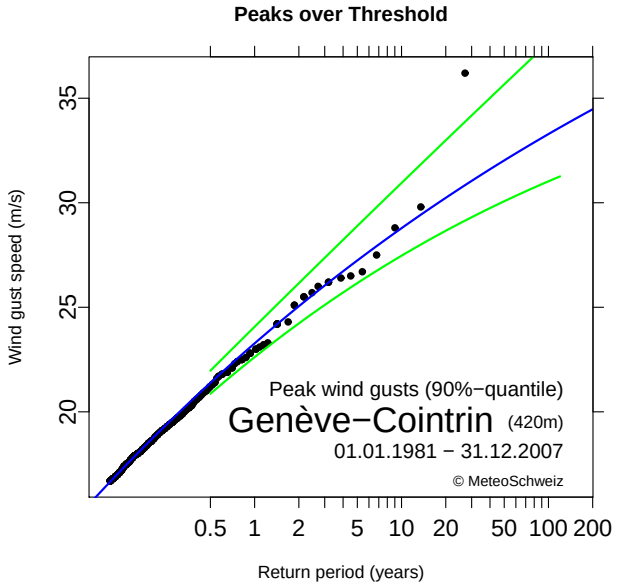

d)

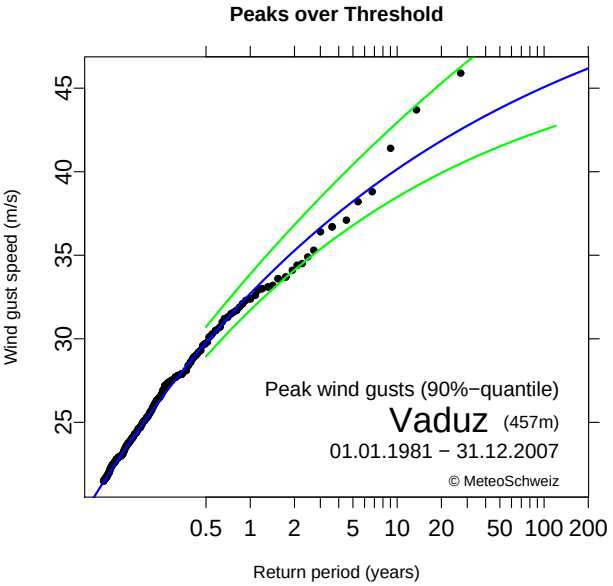

e)

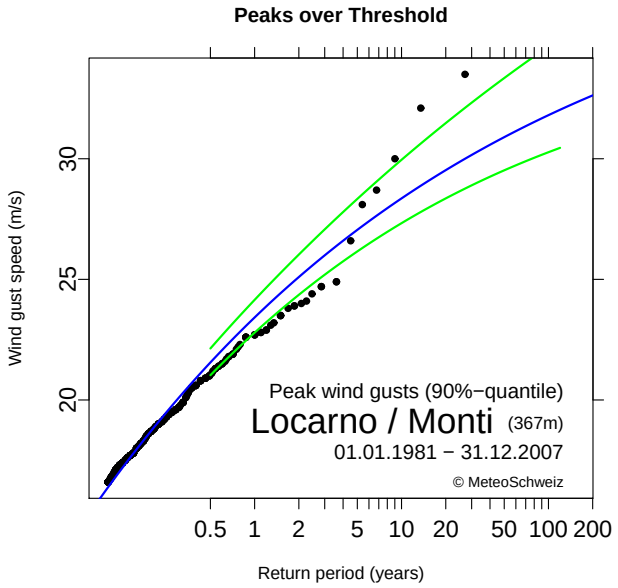

f)

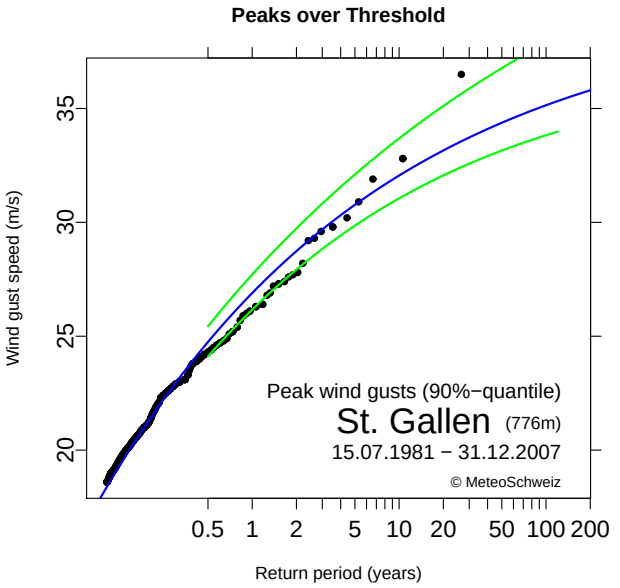

Figure 4.2: As for figure 4.1 for six other stations. For more examples see Appendix A.

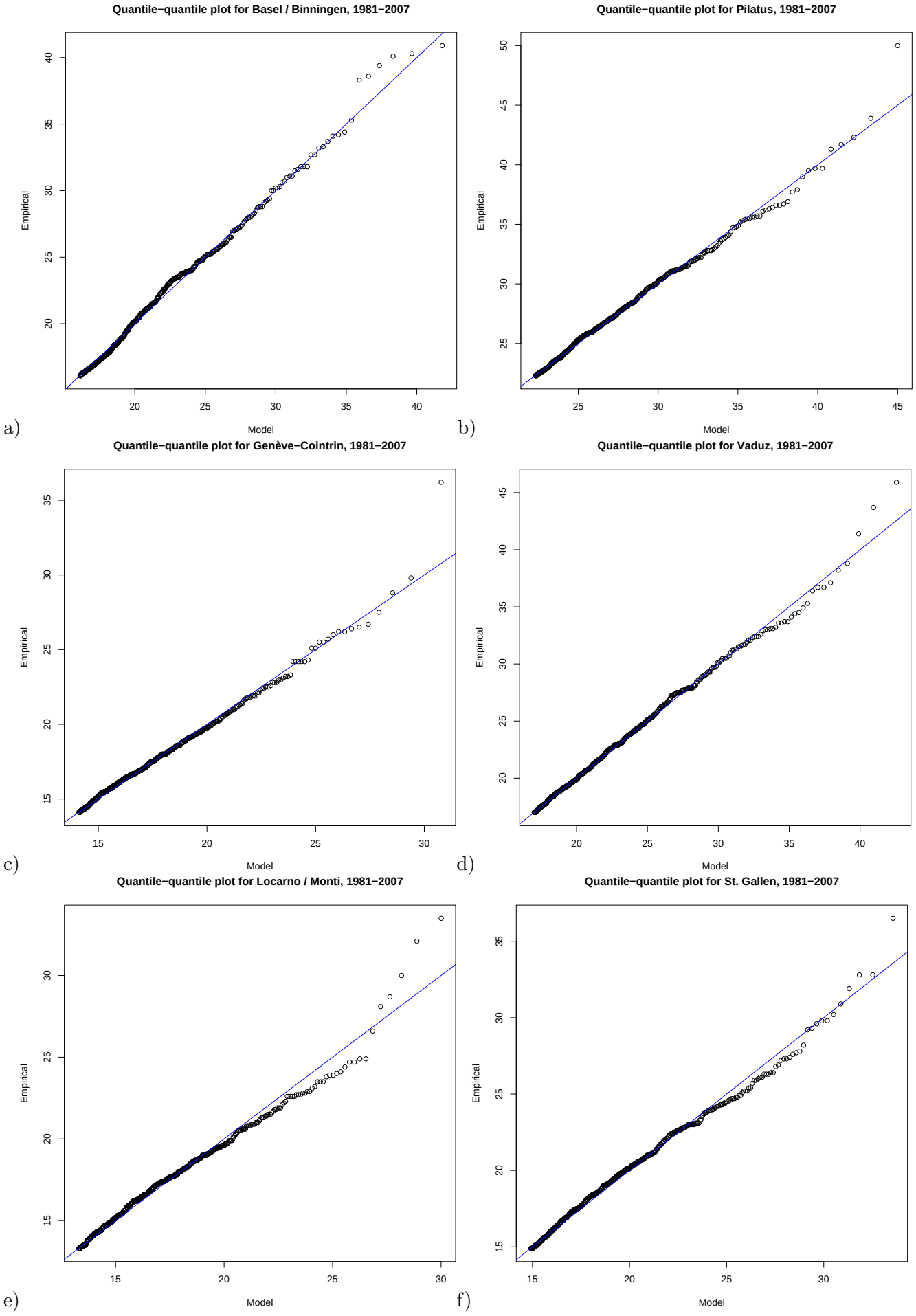

Figure 4.3: Quantile-quantile plots for the six stations shown in figure 4.2.

4.2 Spatial variation of GPD parameters

The POT series is created by declustering peaks above the 90% quantile. For this reason, the threshold varies from one station to another, depending on the local wind climatology. The threshold levels are displayed on figure 4.4. As one could expect, higher thresholds are found at wind-exposed stations, typically mountain stations, with values well above 20 m/s; typical examples are Jungfraujoch, La Dôle or Saentis. Low thresholds are located in the southern Plateau as well as in central Valais and in Ticino valleys, corresponding to less wind-exposed stations / regions. The lowest values for all Switzerland are observed in Southern Ticino (Stabio) and in the upper Rhine Valley (Disentis / Sedrun).

The shape parameter ξ, which defines the behaviour of the tail of the GPD, shows relatively little spatial variation. Its value is negative at all stations but one (see figure 4.5), and in general the values are comprised between 0 and -0.2. In other words, the shape of the GPD fit is quite similar at all stations. A possible interpretation of this property is that the physical constraints that detemine the shape of the extreme wind distribution are similar everywhere.

As for the scale parameter σ, which measures the scale or "variability" of the distribution, one expects it to be higher at wind-exposed stations, because the spread of the return values should be larger at the stations which feature the highest wind gusts. Figure 4.6 shows this is the case, and comparison with figure 4.4 indicates that the scale parameter is also correlated with the threshold levels.

Finally, figure 4.7 shows the spatial distribution of the lambda parameter (λ), which indicates the mean number of peaks per year. This parameter also features some regional differences, with wind-exposed stations having smaller lambdas. We believe the variation is due to the differences in the auto-correlation of wind speed between the stations. High autocorrelation results in less peaks being chosen by the declustering method, and thus in a shorter peak series. If this is the case, this would mean that the wind gust series have a higher auto-correlation at wind-exposed stations.

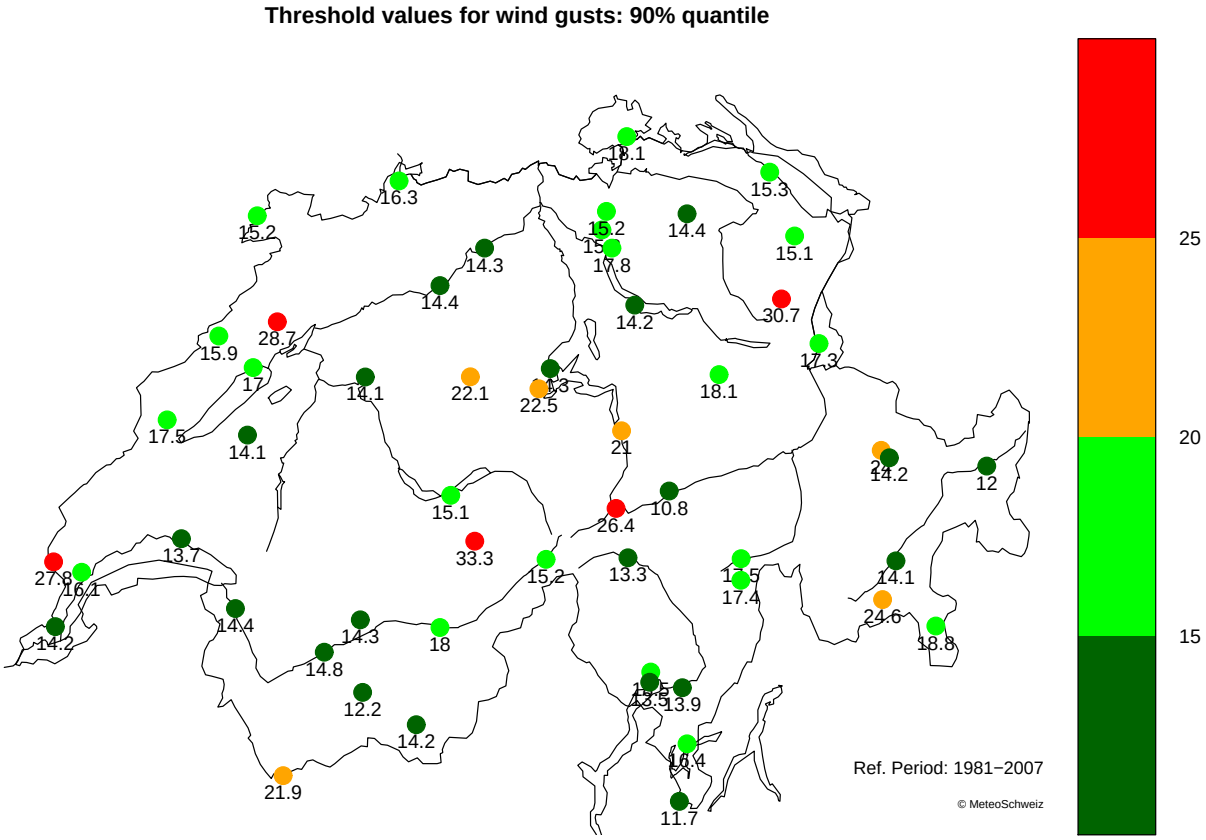

Figure 4.4: Spatial distribution of threshold values (in m/s).

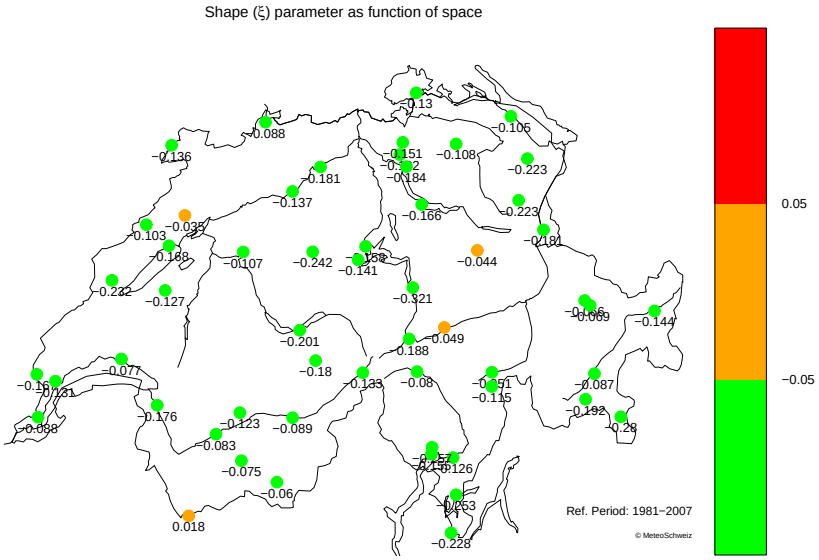

Figure 4.5: Spatial distribution of the shape parameter (ξ).

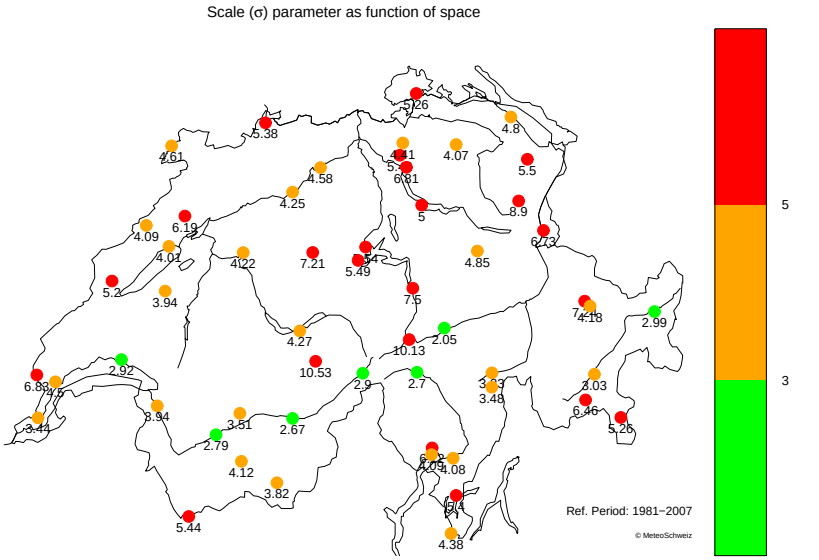

Figure 4.6: Spatial distribution of the scale parameter (σ).

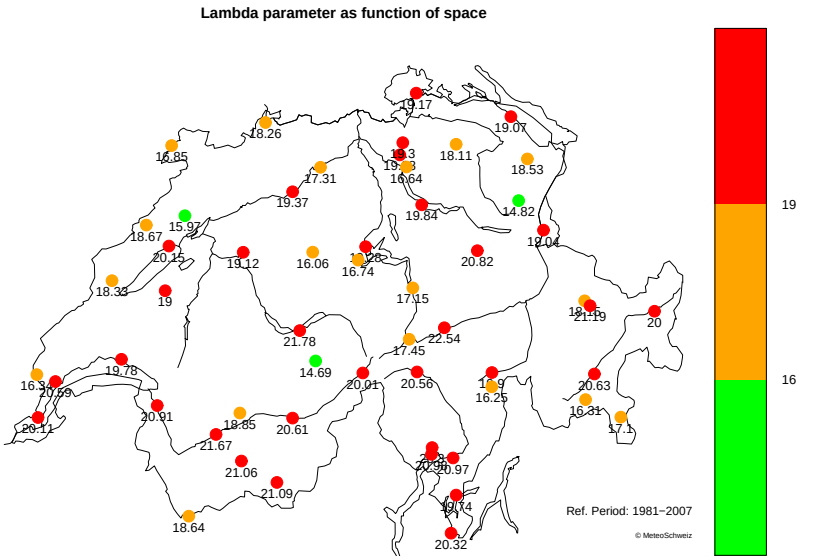

Figure 4.7: Spatial distribution of the lambda parameter (λ).

4.3 Return levels and return periods

4.3.1 Return periods of given wind speeds

An interesting application of our results lies in the possibility of estimating the return period of any given wind gust speed. Of course, these estimates are associated with uncertainties, but for not too extreme wind gust speeds the confidence intervals are reasonably small. Because of these uncertainties we only display ranges of RP values and not the exact values; the ranges are represented with a colour code. We chose to investigate the return period of wind gusts of 25, 30 and 35 m/s (90, 108 and 126 km/h respectively). The results are shown on figure 4.8.

The plots indicate that the distribution of extreme winds is very inhomogeneous, since the return periods range from <2 to 100+ years. We see that for most stations, wind gusts of 25 m/s are not exceptional, with most return periods being lower than 2 years. The frequency of gusts of 30 m/s, however, is very variable. Wind-exposed stations can be easily identified because of the low return periods; as could be expected, the highest return periods are situated in regions that are protected from high wind speeds, such as some inner alpine valleys. Finally, wind gusts of 35 m/s are extreme events almost everywhere, except for very wind-exposed stations. Notice that a few stations in the northern Swiss plateau feature relatively low return periods (<5 years), namely Zürich / Fluntern, Schaffhausen and Basel / Binningen; this is also the case for stations in Föhn valleys, such as Altdorf and Vaduz.

4.3.2 Return levels of given return periods

In this section we analyse the spatial variability of the return levels (RLs) of given return periods (RPs); for this we consider RPs of 2, 5, 10 and 50 years (see figure 4.9). As in previous plots, we can notice here again the differences in wind exposure: the most wind-exposed stations have the highest return levels. In the following we make a few comments on figures 4.9 b) and d). We can see that the 5-year return levels for most lowland stations on the Swiss Plateau and in Valais are comprised between 25 and 30 m/s. The 50-year return levels are more heterogeneous, with values generally between 30 and 40 m/s. Note that the uncertainty (and thus the confidence intervals) of the RL estimates increase with the RP; in particular, a RP of 50 years, which corresponds to a very extreme event, is associated with very large confidence intervals. For this reason, the RL estimates should be interpreted with caution.

a)

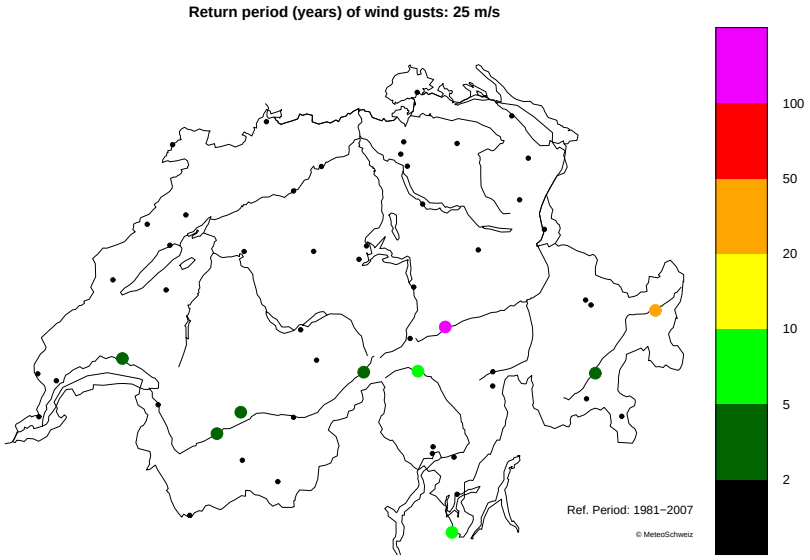

b)

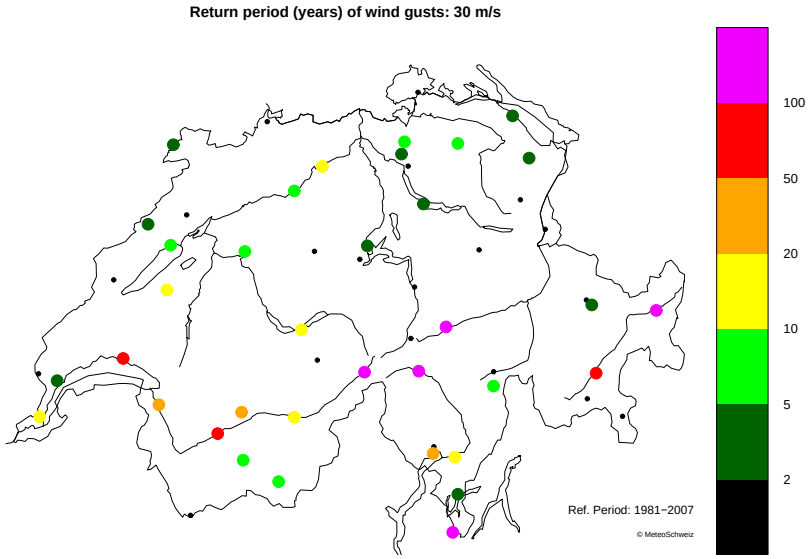

c)

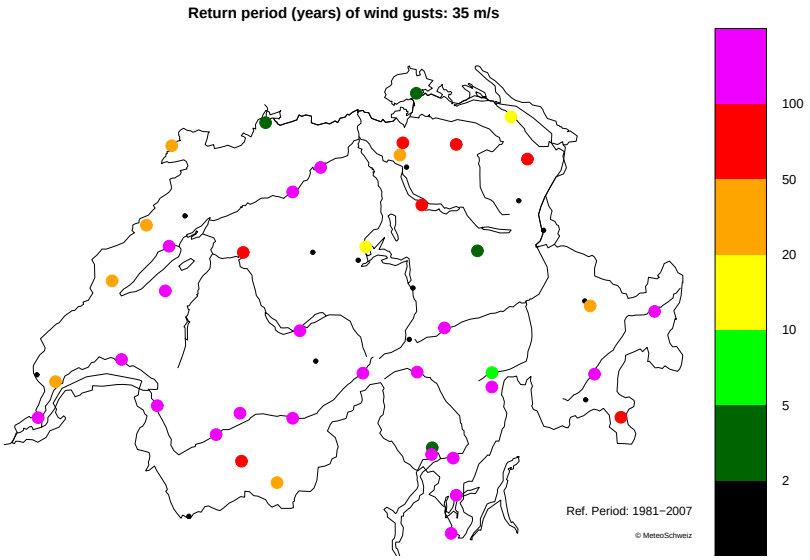

Figure 4.8: Return period of wind gusts of a) 25, b) 30 and c) 35 m/s.

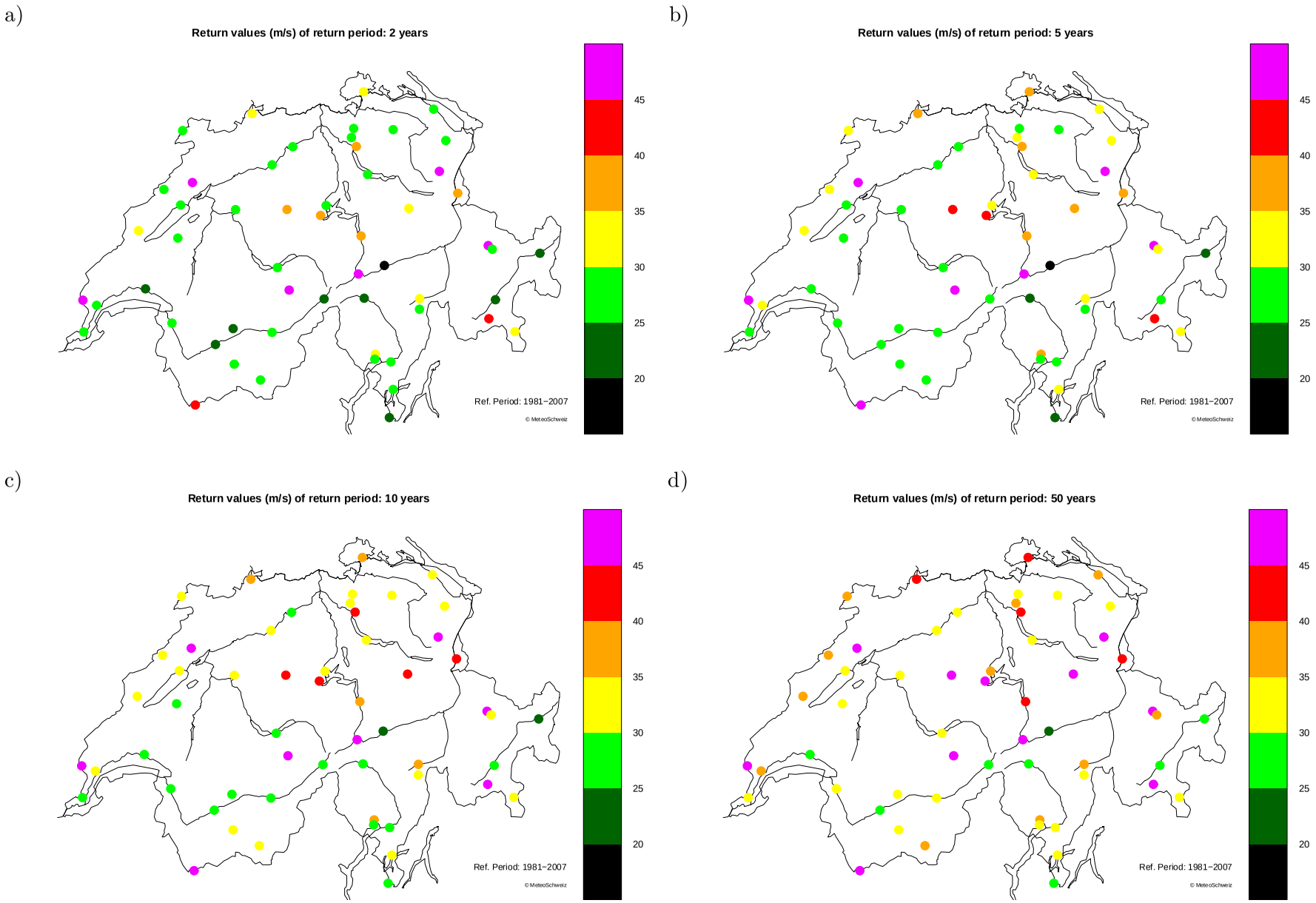

Figure 4.9: RLs corresponding to RPs of a) 2, b) 5, c) 10 and d) 50 years.

4.4 Return period of some prominent wind storms

We investigated the return periods of five significant wind storms that affected Switzerland over the last three decades. We considered the following storms: Lothar (26 December 1999), Wilma (26 January 1995), Vivian (27 February 1990), an unnamed storm (24 March 1986), and a Föhn storm (8 November 1982). Some of these storms were selected using the return periods in Della-Marta et al. (2008), figure 14. The results are shown on figures 4.10 - 4.12.

The first striking feature is that Lothar was a very extreme event. At many stations, the return period lies above 100 years, especially in the northern Swiss Plateau; only Ticino and Graubünden were not affected. Albisser et al. (2001) performed a detailed analysis of this event. They showed that Lothar was most extreme in the central and eastern Prealps as well as in central and northern Switzerland; in particular, they pointed out extreme wind gusts in the Brienz region (50 m/s). On the other hand, inner alpine regions were not affected. The general extreme wind distribution is reflected quite well in our results; however, the spatial resolution of our analysis is too low for a detailed comparison with the results from Albisser et al. (2001).

Vivian was also an extreme event, especially in inner alpine regions such as Valais. However, the return periods are generally slightly lower than in the Lothar case. Our results match the observations from Albisser et al. (2001), who also noted that compared to Lothar, Vivian had more impact in the inner Alps, and generated slightly less extreme wind gusts at most stations. A peculiarity of the storms Lothar and Vivian lies in the fact that they affected almost all regions on the northern side of the Alps, including some alpine valleys. Thus, they were exceptional not only with regard to their intensity, but also because of their spatial extension. The two other west wind storms we represented (figures 4.10 b) and 4.11 b)) also generated very extreme winds, but seem to have had a more limited effect: only regions that are well-exposed to westerly winds were concerned.

In general, regional differences are well represented in the plots, and it is easy to distinguish which regions are most affected by each storm. The four first examples are west wind storms, which hit especially the north side of the Alps. The Föhn storm (figure 4.12) only affected Föhn-exposed alpine valleys. We notice that not all Föhn valleys were affected in the same manner: the event was much more extreme in Lower Valais than in other regions. The magnitude of the Föhn event in a particular valley probably depends on the direction of the flow as well as on other local effects which are difficult to predict. In general, however, the return periods of this Föhn event are not very extreme. Other particularly strong Föhn events did not feature very extreme return periods, either (results not shown). Our hypothesis for this observation is that Föhn storms are characterised by very strong *mean* winds; the related wind gusts, however, are not particularly extreme.

A general feature of the plots is that the spatial distribution of the return periods of a particular storm is very inhomogeneous. In other words, an extreme wind event at one station may not be (as) extreme somewhere else. At some stations, Lothar is the most extreme event whereas at others, it is Vivian, Wilma or even another storm. This confirms what we already know about extreme winds: they are subject to many complex, small-scale phenomena which produce large differences over small distances. However, this analysis enables us to make the best possible estimation of the intensity and the spatial extension of a particular storm, given the limitations in the length of records and their spatial density.

a)

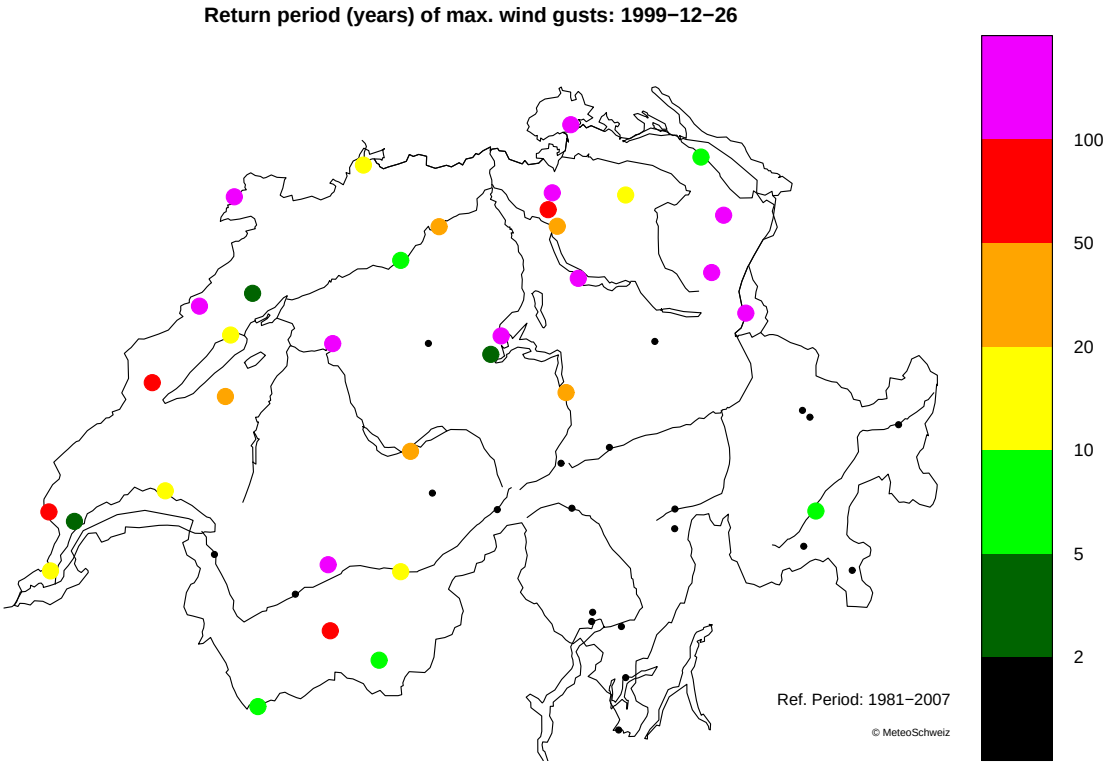

b)

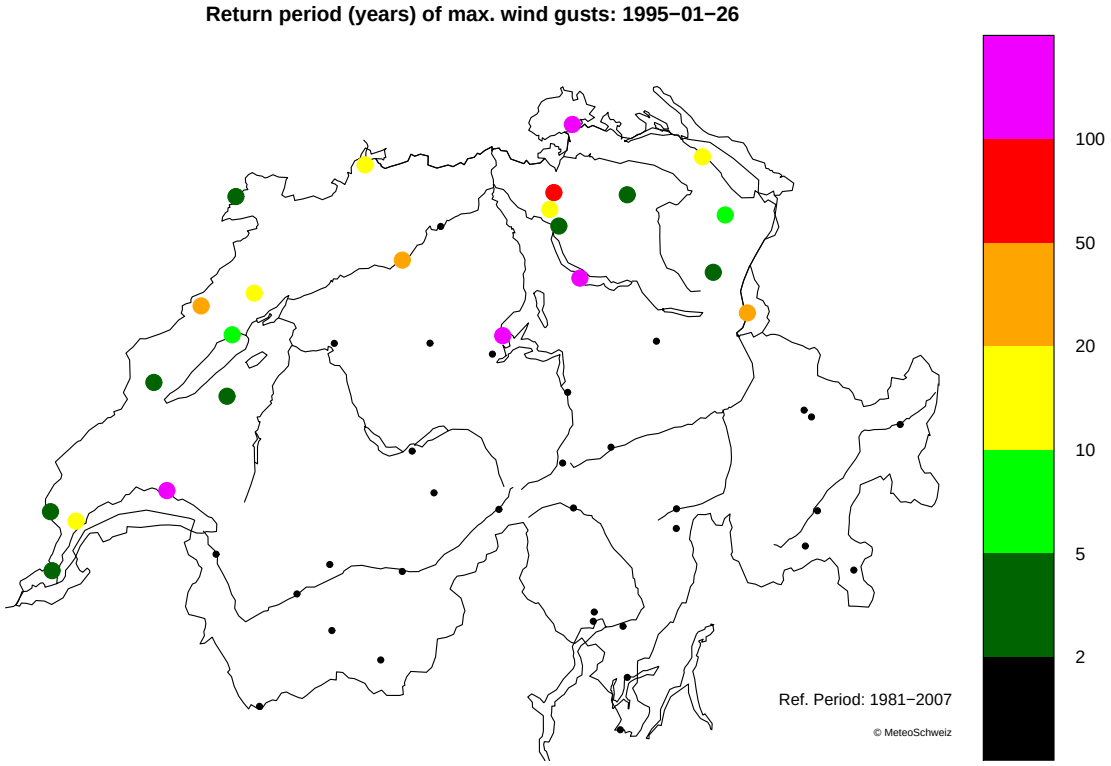

Figure 4.10: Return periods (in years) of storms a) Lothar (26 December 1999) and b) Wilma (26 January 1995).

a)

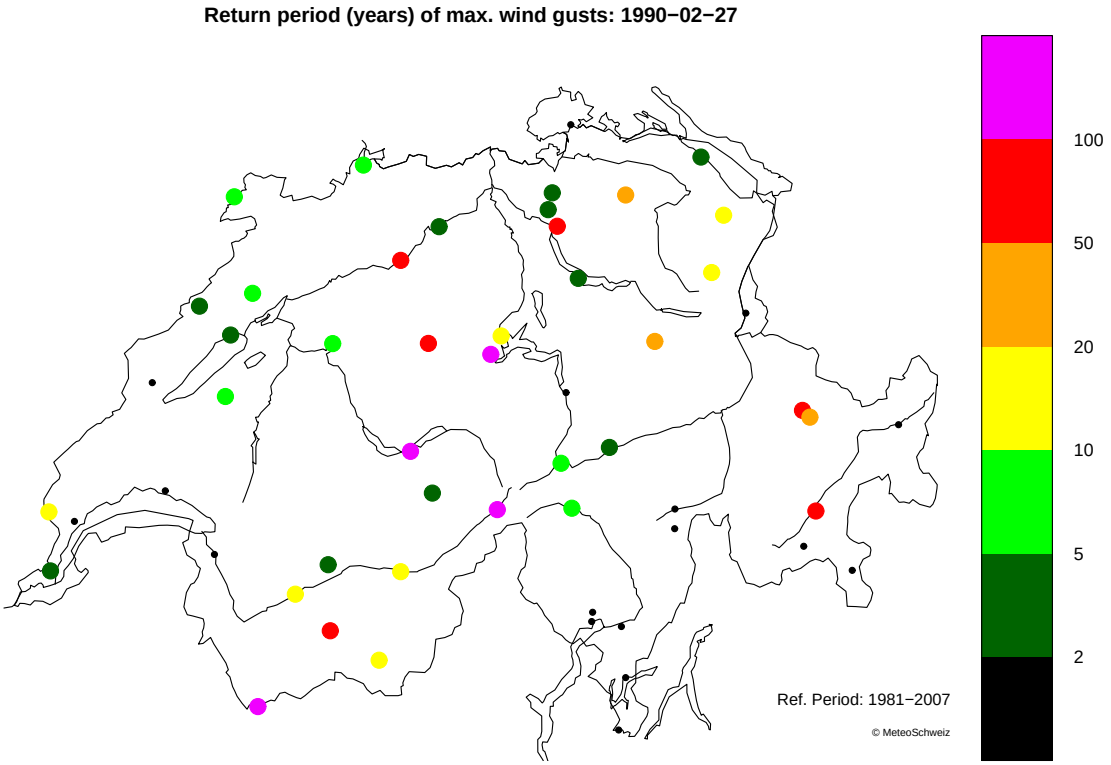

b)

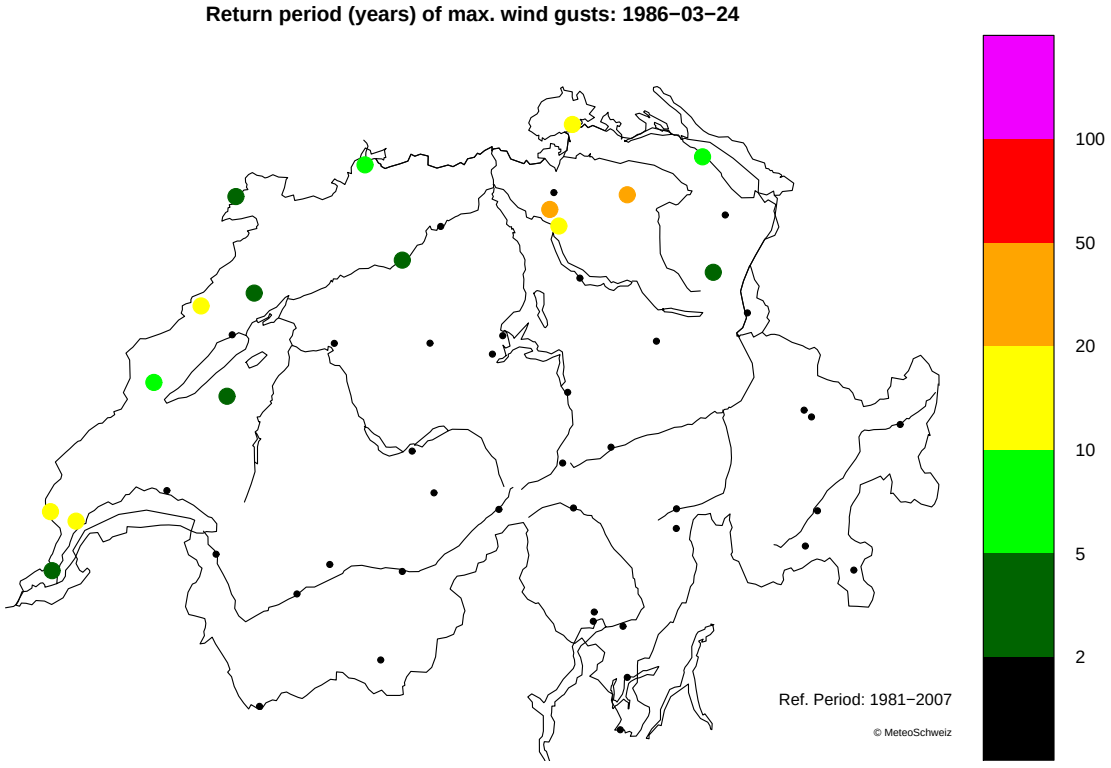

Figure 4.11: As for figure 4.10 for a) storm Vivian (27 February 1990) and b) an unnamed storm (24 March 1986).

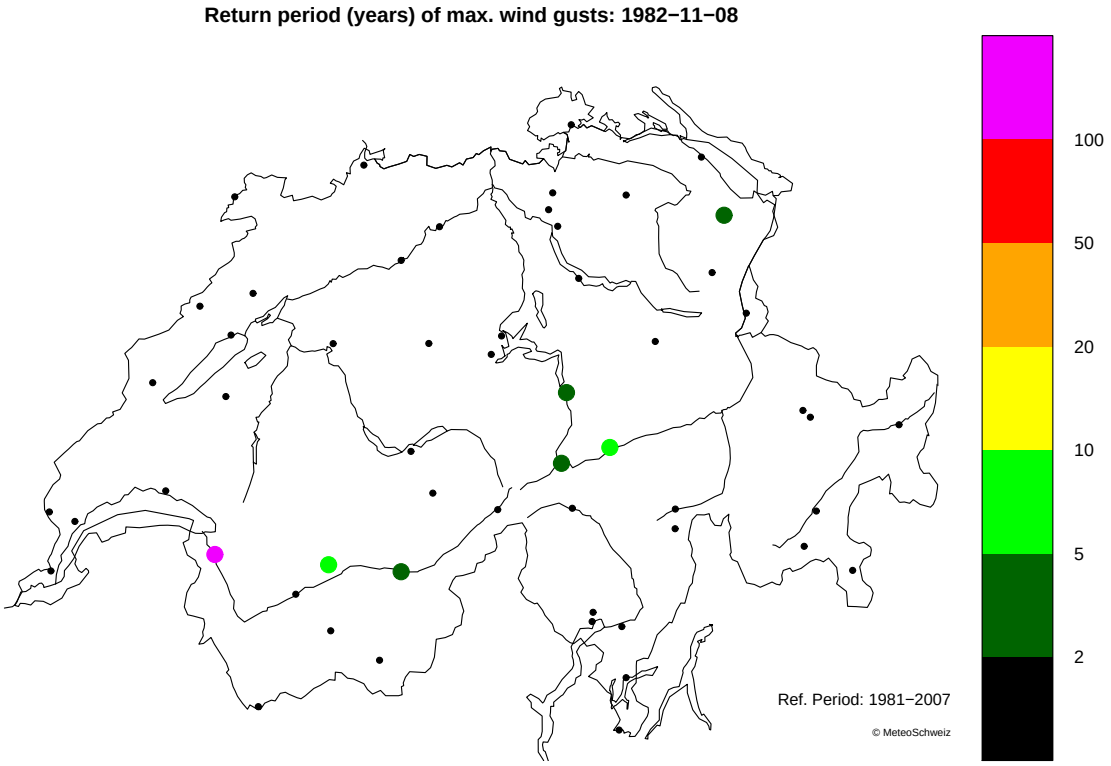

Figure 4.12: Return periods of an unnamed Föhn storm (8 November 1982).

4.5 Block Maxima method and comparison with POT analysis

POT is not the only appropriate method for statistical analysis of extreme values. Another commonly used possibility is the *Block Maxima* approach. In this section we want to briefly introduce this method and compare its results with our POT analysis.

In the Block Maxima method the extremes are chosen as *maximum values* of large *blocks* of data - hence the name "Block Maxima". As in the POT approach, these maxima are then used for a parametric estimation of a probability distribution function. This function is called a *Generalised Extreme Value Distribution* (GEV) and is a cumulative density function. It can be expressed as follows:

$$G(x) = \exp\left\{1 - \left[1 + \frac{\xi}{\sigma}(x-u)\right]^{-\frac{1}{\xi}}\right\} \tag{4.1}$$

where the function parameters ξ and σ have the same meaning as in the GPD function (see equation 3.1). With this probability distribution function a return value function can be calculated in the exact same way as in the POT case. The estimation of the GEV function parameters and of the confidence intervals is also performed using the same methods as for the GPD function (see sections 3.2 and 3.4).

As in the POT method, we must assume that the extremes are independent and identically distributed. In our context (extreme wind analysis) this requires a block size of one year in order to eliminate seasonality effects. As we have only 27 years available in our dataset, this means the parameters of the GEV function have to be estimated with as little as 27 values. This is one of the main reasons for choosing the POT method for our extreme value analysis. Indeed, the POT approach utilises much more information from the distribution of peaks, leading to a more accurate estimation of the return value function; this is reflected in the confidence intervals, which are smaller in the POT estimation than in the Block Maxima method (see figure 4.13).

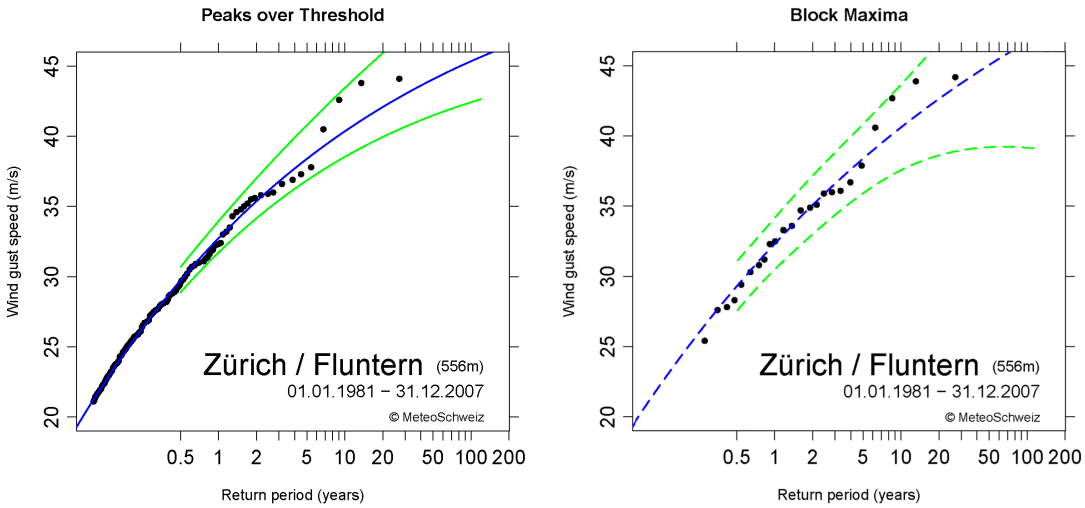

Figure 4.13: Comparison between the GPD fit (left) and the GEV model fit (right)

	GPD	GEV
Shape ξ	-0.18	-0.13
Scale σ	6.81	4.26

Table 4.1: Parameters of the GPD and GEV models at station Zürich / Fluntern.

We performed a quick Block Maxima analysis to ten stations from our dataset in order to compare the two extreme value analysis methods. As an example we compare the two models for the station Zürich / Fluntern (figure 4.13). One of the main differences lies in the fact that the shape parameter is less negative in the GEV case (see table 4.1) - in other words, the curve is less concave. This leads to significantly lower return period estimates for high wind speeds with the GEV model; the values shown on table 4.2 indicate that the differences become large above 40 m/s, i.e. for extreme events. We observed this feature for all of the stations we analysed with the Block Maxima method. Hence, this approach provides relatively low return periods for extreme storms such as Lothar or Vivian. Table 4.3 shows a comparison of the return period estimates for the four west wind storms represented on figures 4.10 and 4.11.

a) GPD model

Return level [m/s]	Return period [years]
34	1.4
36	2.4
38	4.4
40	8.8
44	48.5
46	147.6
50	3967.8

b) GEV model

Return level [m/s]	Return period [years]
34	2.2
36	3.3
38	5.3
40	9.3
44	35.2
46	77.6
50	522.1

Table 4.2: Comparison of the return periods obtained from a) the GPD and b) the GEV model at station Zürich / Fluntern.

	GPD model		GEV model	
Storm name and date	Max. wind gust speed [m/s]	Return period [years]	Max. wind gust speed [m/s]	Return period [years]
Lothar 26.12.1999	43.8	43.9	43.8	32.7
Wilma 26.01.1995	35.8	2.3	35.8	3.1
Vivian 27.02.1990	44.1	51.0	44.1	36.6
unnamed 24.03.1986	40.5	10.6	40.5	10.8

Table 4.3: As in table 4.2 for the four storms displayed on figures 4.10 and 4.11.

In their analysis of the Lothar event, Albisser et al. (2001) also performed a Block Maxima analysis for 28 stations. For Zürich / Fluntern their estimated return period was as low as 12 years. However, their analysis was based on only 19 years of measurement records; this might explain the difference compared to our results. This seems to indicate that for too short measurement series the Block Maxima method overestimates the shape parameter, so that it also underestimates the return periods of extreme events. If this is the case, the two approaches (Block Maxima and POT) should give quite similar results for longer time series.

Chapter 5

Discussion and Recommendations for Further Research

5.1 Discussion of the results

One of the main goals of this work was to assess the potential for creating a wind climatology based on in-situ wind gust measurements. Our results have shown that the data quality of most of the time series is very good and that the distribution of the POT series can be modelled well by a GPD model fit. In particular, the quality and length of the data are sufficiently good for an extreme value analysis; the quantile-quantile plots show the model fit was good, with systematic deviations in a few cases only. In other words, it is possible to obtain reliable station-based extreme wind climatologies.

Compared to other studies based on reanalysis model data (Della-Marta et al., 2007, 2008), the advantage of using station data lies in the fact that small-scale effects acting on surface winds can be much better described. Indeed, global reanalysis data for surface wind have biases and are very coarse in resolution; they are thus not be suitable for wind analysis at local space scales.

Our analysis provides information about the RP of local wind gusts at a particular station. However, visual representation of the spatial distribution of the RPs also gives a more general picture about the magnitude of an extreme wind event on a regional scale, and describes how the effects of the storm are distributed in space. Thus, the analysis of storm Lothar showed not only that the intensity of the local wind gusts was extreme, but also that the spatial extension of the extreme gusts was exceptional; the storm was extreme not only at a specific point, but over all of the north side of the Alps. This corresponds well with the analysis made by Albisser et al. (2001).

In the following we want to compare briefly our results with the work done by Della-Marta et al. (2008) based on reanalysis model data. Their parameter estimates were similar to ours, especially with respect to the shape parameter (ξ), with negative values almost everywhere; only a few grid points had slightly positive values. In particular, their wind climatologies over land exhibit shape values in the range -0.33 $\leq \xi \leq$ -0.18, which means that their grid point based GPD fits also had an upper bound. In addition, the distribution of the scale parameter (σ) was similar to that of the threshold levels, grid points with high thresholds displaying wider distributions; this also reflects our results. The lambda parameters cannot be compared because of different time block sizes.

Regarding the RP of specific storms, we also see a good correspondence between the results of the two studies. Their grid point based RP estimates for Lothar also display values close to or above 100 years over much of central Europe. Wind gust analysis of storm Vivian shows RPs in the same order of magnitude as ours as well. However, it is difficult to make a direct comparison between the two studies, since the resolution of the analysis in Della-Marta et al. (2008) is much coarser than ours, so that no accurate RP estimation can be made for Switzerland.

5.2 Recommendations for further research

Due to the requirements of this Bachelor thesis, we had to restrict our EVA to 55 stations with full time series (1981 - 2007). Indeed, the check of the quality and homogeneity of the series was a time consuming step. However, we believe it is necessary to include further stations with shorter measurement series, as 132 stations are available in total. This would provide a better spatial resolution, giving even more information about local differences in extreme wind climatologies together with more reliable RP estimates.

Another possibility lies in the inspection of the quality of the time series. We limited ourselves to analysing the long-term variability of the measurement series, as well as monthly and seasonal averages of the latter. A deeper analysis would be beneficial, as we think quality issues might be the cause for some of the bad GPD fits at certain stations.

The systematic deviations from the GPD fit should also be inspected carefully. We mentioned that all lowland stations in Ticino exhibited this feature. However, we only have four lowland stations in this region, so it would be necessary to include more Ticino stations into the analysis. A question that should be addressed is whether the deviations are due to data quality issues or whether other factors play a role, e.g. climatological factors that might influence the distribution of extreme winds.

Finally, in the extreme value analysis of the wind gusts, the synoptic weather pattern could also be taken into account. Indeed, our analysis is independent from the wind direction. It is known that most extreme wind events - at least on a regional scale - are related to west wind storms (mostly in winter). We believe it might be interesting to take the wind direction into account as this would enable to evaluate the extremeness of other situations, such as Bise winds, independently from the general wind climatology. This would also make it possible to estimate which regions are most affected by each type of general weather pattern.

Appendix A

Extreme wind climatologies

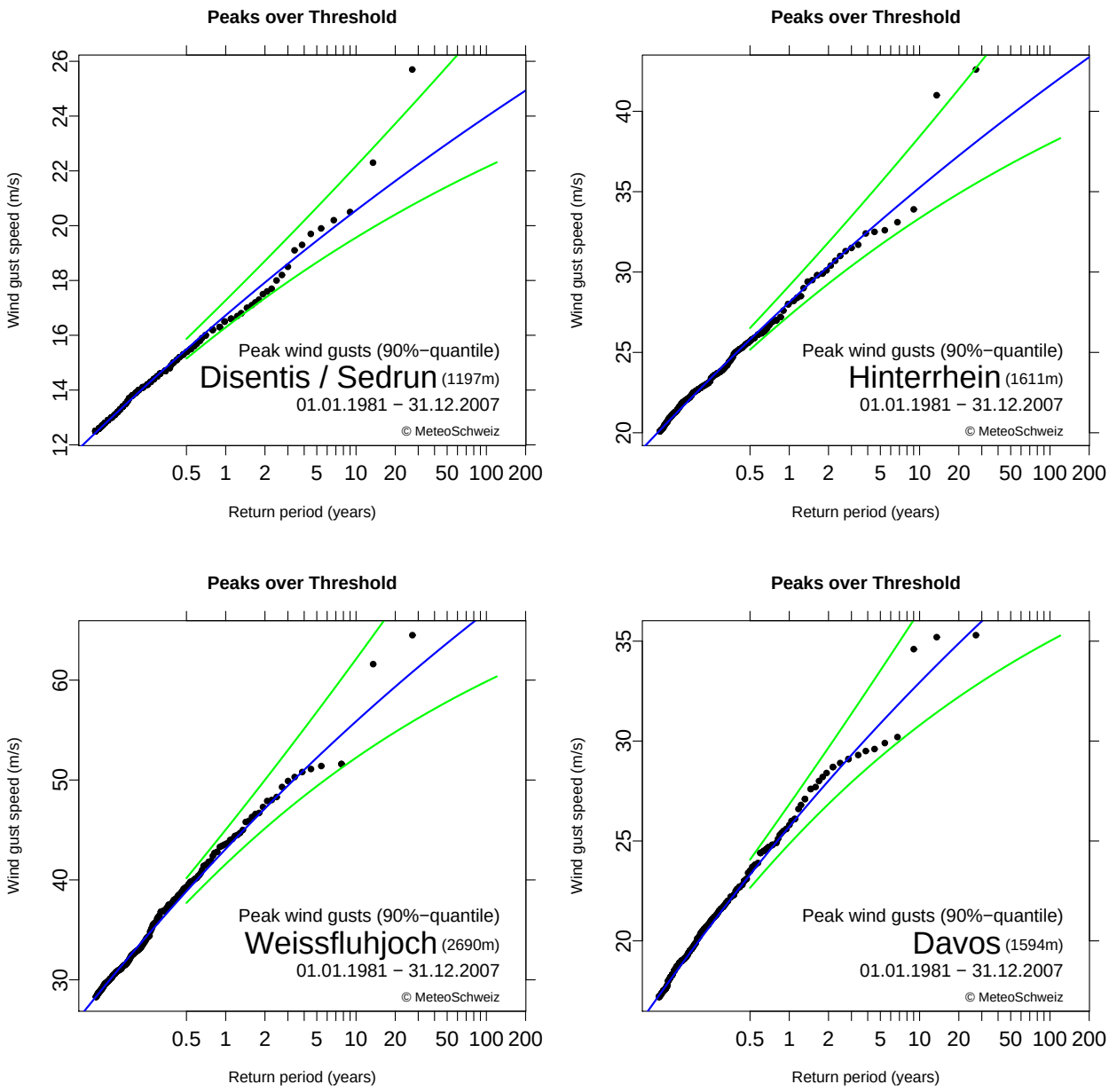

Figure A.1: Extreme wind climatologies. For description see figure 4.1.

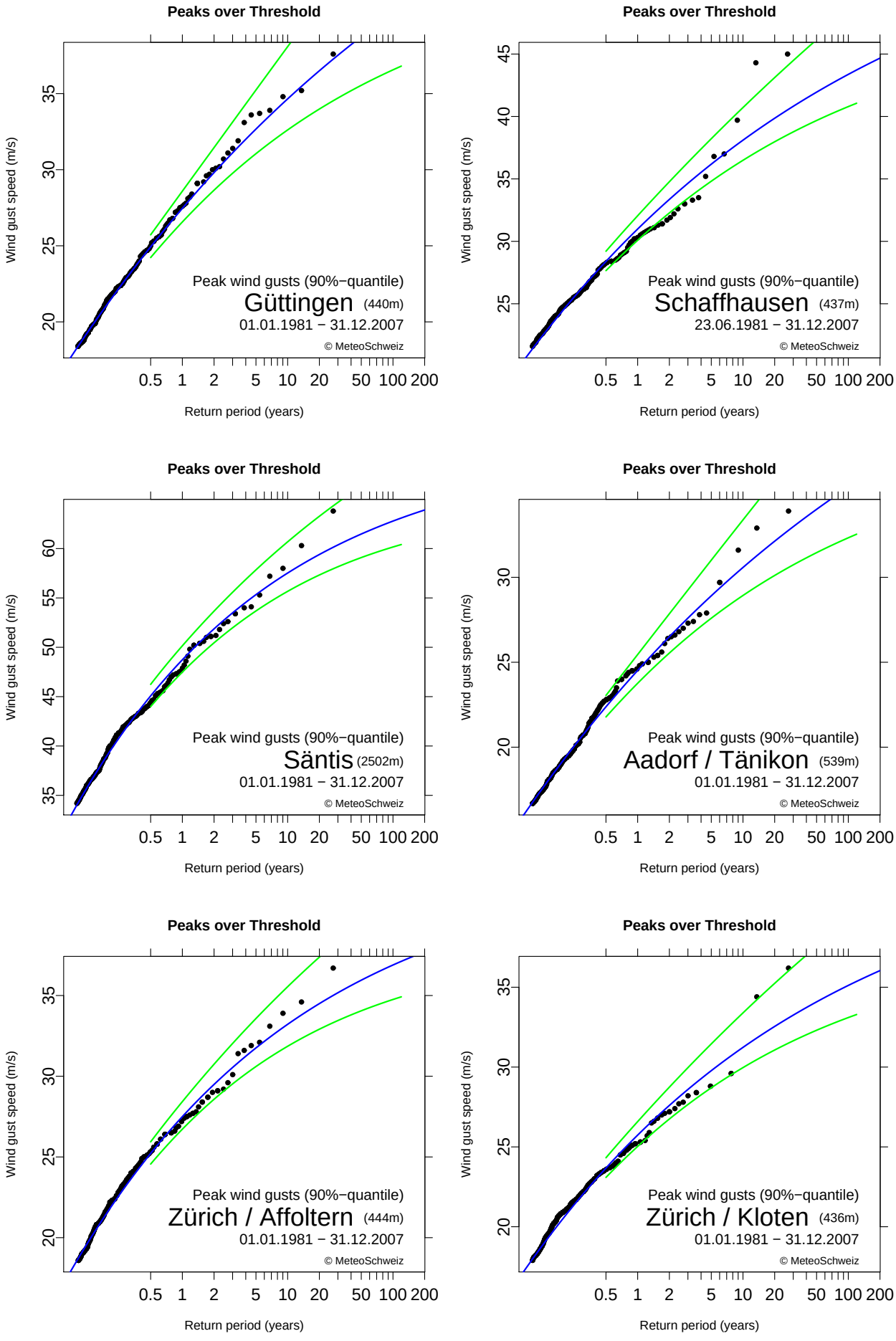

Figure A.2: Extreme wind climatologies. For description see figure 4.1.

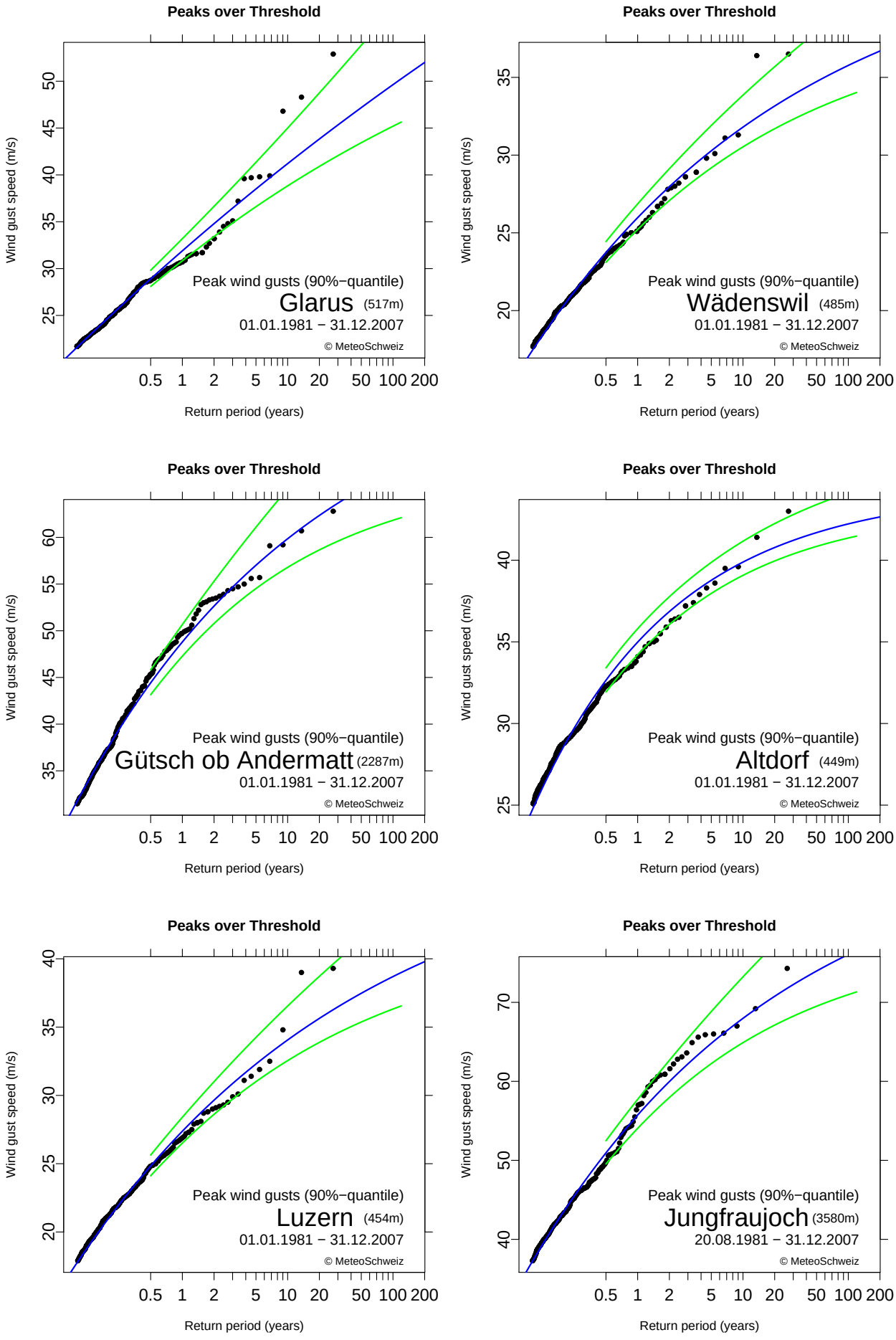

Figure A.3: Extreme wind climatologies. For description see figure 4.1.

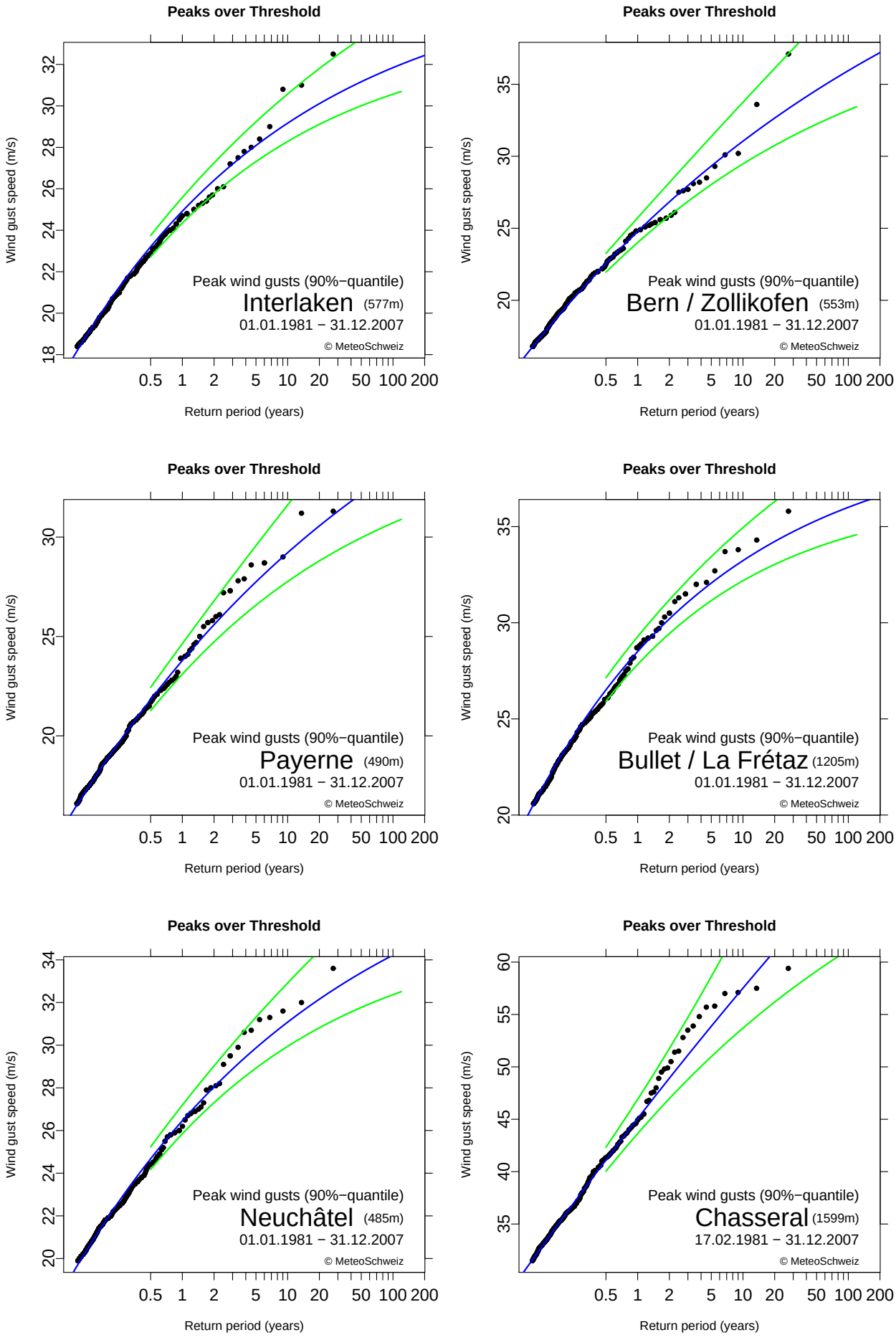

Figure A.4: Extreme wind climatologies. For description see figure 4.1.

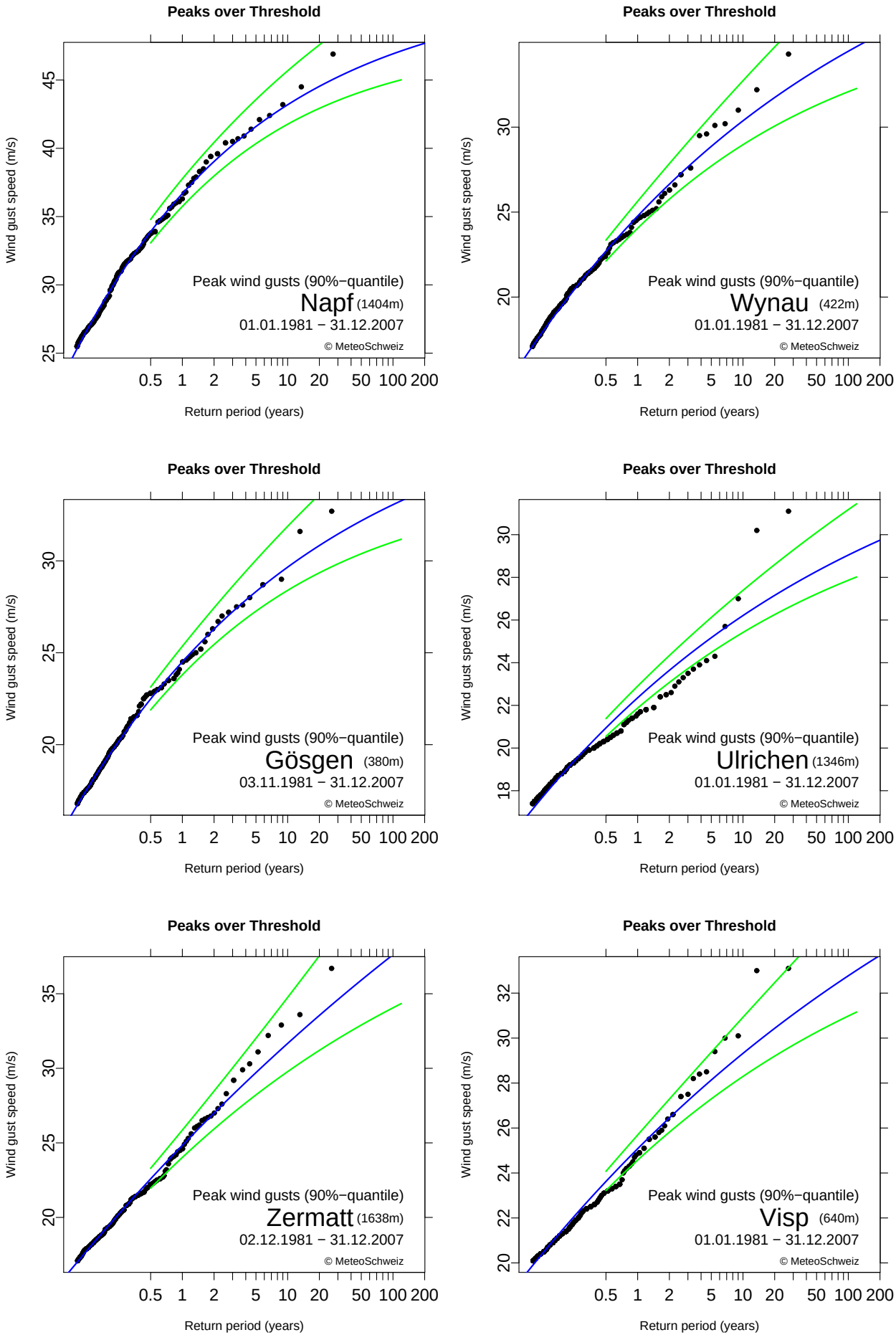

Figure A.5: Extreme wind climatologies. For description see figure 4.1.

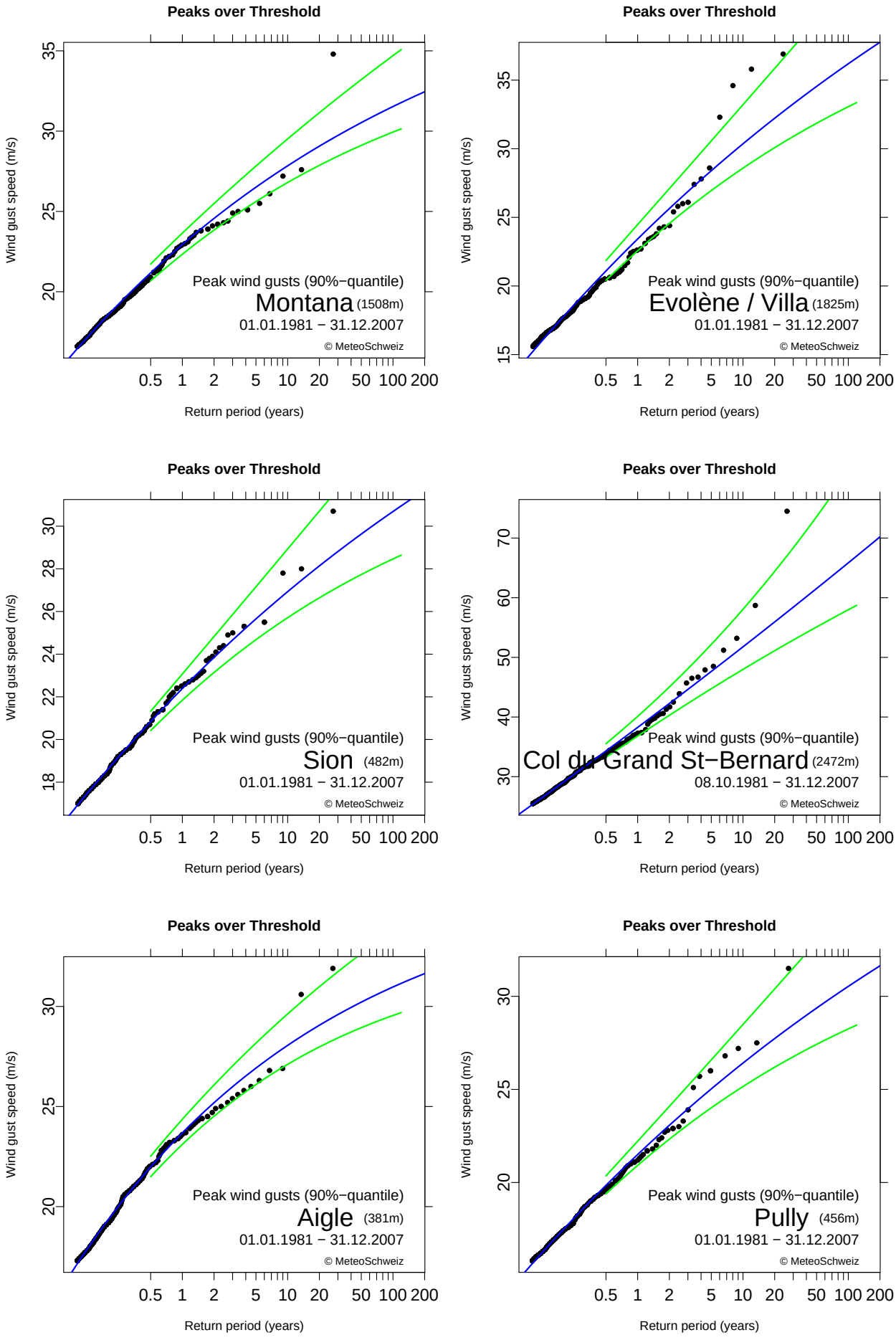

Figure A.6: Extreme wind climatologies. For description see figure 4.1.

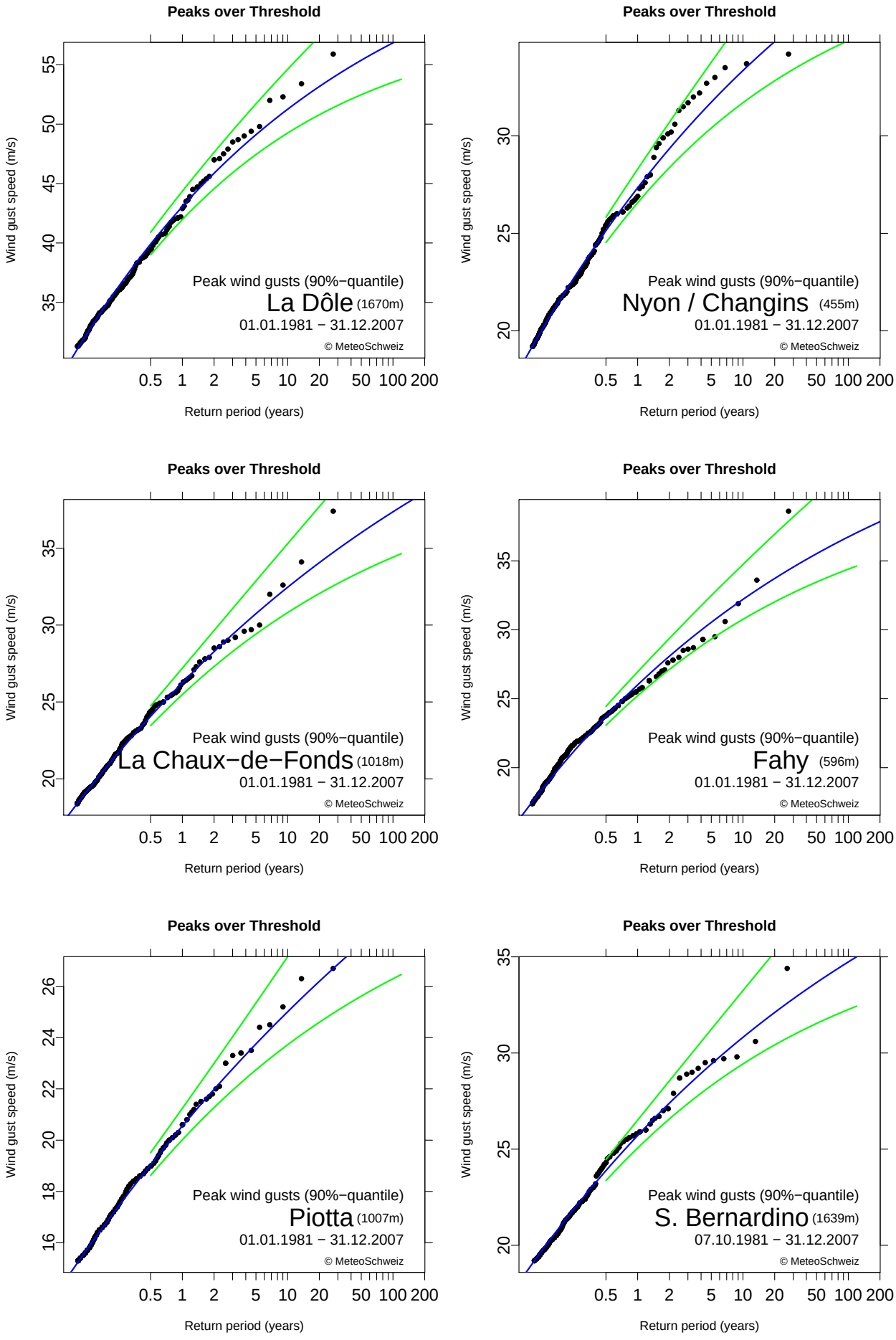

Figure A.7: Extreme wind climatologies. For description see figure 4.1.

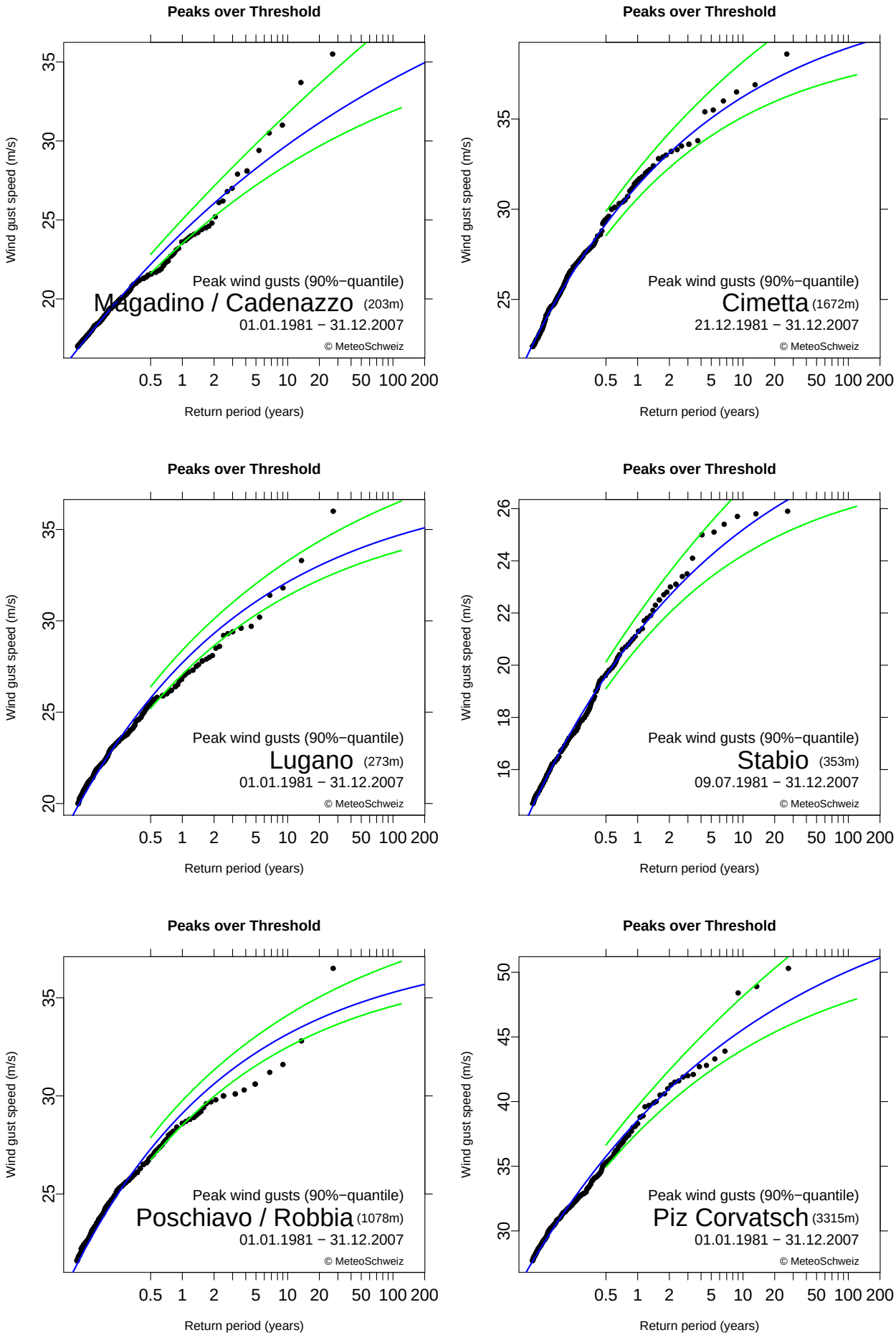

Figure A.8: Extreme wind climatologies. For description see figure 4.1.

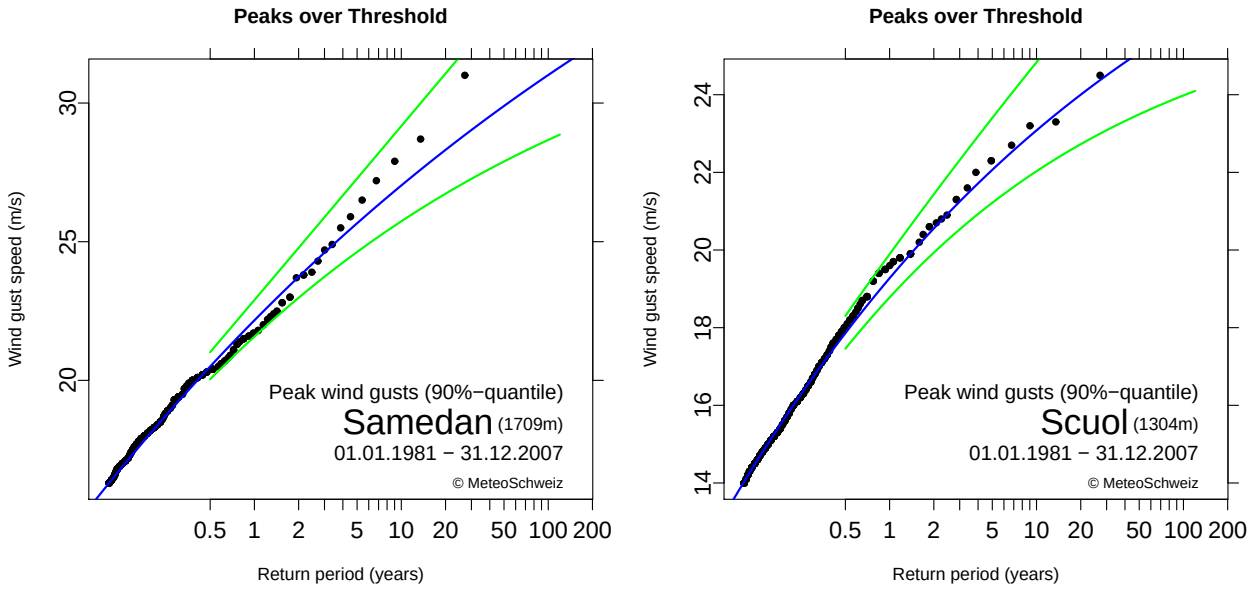

Figure A.9: Extreme wind climatologies. For description see figure 4.1.

Bibliography

P. Albisser, D. Aller, S. Bader, P. Brnag, A. Broccard, A. Bründl, M. Dobbertin, B. Forster, F. Frutig, P. Hächler, T. Hänggli, C. Jacobi, E. Müller, U. Neu, S. Niemeyer, C. J. Nöthiger, J. Quiby, C. Rickli, A. Schilling, F. Schibiger, and G. Truog. *Lothar Der Orkan 1999*. Eidg. Forchungsanstalt WSL, Bundesamt für Umwelt, Wald und Landschaft BUWAL, Birmensdorf, Bern., 2001.

S. Coles. *An introduction to statistical modeling of extreme values*. Springer, 2001.

P. M. Della-Marta, H. Mathis, C. Frei, M. A. Liniger, and C. Appenzeller. Extreme wind storms over europe: Statistical analyses of ERA-40. Technical report, Federal office for Meteorology and Climatology, MeteoSwiss, Arbeitsbericht 216, 2007.

P. M. Della-Marta, H. Mathis, C. Frei, M. A. Liniger, J. Kleinn, and C. Appenzeller. The return period of wind storms over Europe. *International Journal of Climatology*, Submitted, 2008.

R. A. Fisher and L. H. C. Tippett. Limiting forms of the frequency distribution of the largest or smallest member of a sample. *Proceedings of the Cambridge Philosophical Society*, 24:180–190, July 1928.

E. S. Martins and J. R. Stedinger. Generalized maximum-likelihood generalized extreme-value quantile estimators for hydrologic data. *Water Resources Research*, 36(3):737–744, March 2000.

J. P. Palutikof, B. B. Brabson, D. H. Lister, and S. T. Adcock. A review of methods to calculate extreme wind speeds. *Meteorological Applications*, 6(2):119–132, June 1999.

H. Wernli, S. Dirren, M. A. Liniger, and M. Zillig. Dynamical aspects of the life cycle of the winter storm 'lothar' (24-26 december 1999). *Quarterly Journal of the Royal Meteorological Society*, 128(580):405–429, January 2002.

Arbeitsberichte der MeteoSchweiz

218 MeteoSchweiz (Hrsg): 2008, Klimaszenarien für die Schweiz – Ein Statusbericht, 50pp, CHF 69.-

217 Begert M: 2008, Die Repräsentativität der Stationen im Swiss National Basic Climatological Network (Swiss NBCN), 40pp, CHF 66.-

216 Della-Marta PM, Mathis H, Frei C, Liniger MA, Appenzeller C: 2007, Extreme wind storms over Europe: Statistical Analyses of ERA-40, 80pp., CHF 75.-

215 Begert M, Seiz G, Foppa N, Schlegel T, Appenzeller C, Müller G: 2007, Die Überführung der klimatologischen Referenzstationen der Schweiz in das Swiss National Climatological Network (Swiss NBCN), 47 pp., CHF 68.-

214 Schmucki D., Weigel A., 2006, Saisonale Vorhersage in Tradition und Moderne: Vergleich der "Sommerprognose" des Zürcher Bööggs mit einem dynamischen Klimamodell, 46pp, CHF 68.-

213 Frei C: 2006, Eine Länder übergreifende Niederschlagsanalyse zum August Hochwasser 2005. Ergänzung zu Arbeitsbericht 211, 10pp, CHF 59.-

212 Z'graggen, L: 2006, Die Maximaltemperaturen im Hitzesommer 2003 und Vergleich zu früheren Extremtemperaturen, 74pp, CHF 75.-

211 MeteoSchweiz: 2006, Starkniederschlagsereignis August 2005, 63pp., CHF 72.-

210 Buss S, Jäger E and Schmutz C: 2005: Evaluation of turbulence forecasts with the aLMo, 58pp, CHF 70.–

209 Schmutz C, Schmuki D, Duding O, Rohling S: 2004, Aeronautical Climatological Information Sion LSGS, 77pp, CHF 25.–

208 Schmuki D, Schmutz C, Rohling S: 2004, Aeronautical Climatological Information Grenchen LSZG, 73pp, CHF 24.–

207 Moesch M, Zelenka A: 2004, Globalstrahlungsmessungen 1981-2000 im ANETZ, 83pp, CHF 26.–

206 Schmutz C, Schmuki D, Rohling S: 2004, Aeronautical Climatological Information St.Gallen LSZR, 78pp, CHF 25.–

205 Schmutz C, Schmuki D, Ambrosetti P, Gaia M, Rohling S: 2004, Aeronautical Climatological Information Lugano LSZA, 81pp, CHF 26.–

204 Schmuki D, Schmutz C, Rohling S: 2004, Aeronautical Climatological Information Bern LSZB, 80pp, CHF 25.–

203 Duding O, Schmuki D, Schmutz C, Rohling S: 2004, Aeronautical Climatological Information Geneva LSGG, 104pp, CHF 31.–

202 Bader S: 2004, Tropische Wirbelstürme – Hurricanes –Typhoons – Cyclones, 40pp, CHF 16.-

201 Schmutz C, Schmuki D, Rohling S: 2004, Aeronautical Climatological Information Zurich LSZH, 110pp, CHF 34.-

200 Bader S: 2004, Die extreme Sommerhitze im aussergewöhnlichen Witterungsjahr 2003, 25pp, CHF 14.-

199 Frei T, Dössegger R, Galli G, Ruffieux D: 2002, Konzept Messsysteme 2010 von MeteoSchweiz, 100pp, 32 Fr.

198 Kaufmann P: 2002, Swiss Model Simulations for Extreme Rainfall Events on the South Side of the Alps, 40pp, 20 Fr.

197 WRC Davos (Ed): 2001**,** IPC - IX, 25.9. - 13.10.2000, Davos, Switzerland**,** 100pp, 32 Fr.

Frühere Veröffentlichungen und Arbeitsberichte finden sich unter
www.meteoschweiz.ch » Forschung » Publikationen

Veröffentlichungen der MeteoSchweiz

77 Rossa AM: 2007, MAP-NWS – an Optional EUMETNET Programme in Support of an Optimal Research Programme, *Veröffentlichung MeteoSchweiz,* **77,** 67 pp., CHF 73.-

76 Baggenstos D: 2007, Probabilistic verification of operational monthly temperature forecasts, *Veröffentlichung MeteoSchweiz,* **76,** 52 pp.,CHF 69.-

75 Fikke S, Ronsten G, Heimo A, Kunz S, Ostrozlik M, Persson PE, Sabata J, Wareing B, Wichura B, Chum J, Laakso T, Säntti K, Makkonen L: 2007, COST 727: Atmospheric Icing on Structures Measurements and data collection on icing: State of the Art, 110pp, CHF 83.-

74 Schmutz C, Müller P, Barodte B: 2006, Potenzialabklärung für Public Private Partnership (PPP) bei MeteoSchweiz und armasuisse Immobilien, 82pp, CHF 76.-

73 Scherrer SC: 2006, Interannual climate variability in the European and Alpine region, 132pp, CHF 86.-

72 Mathis H: 2005, Impact of Realistic Greenhouse Gas Forcing on Seasonal Forecast Performance, 80pp, CHF 75.

71 Leuenberger D: 2005, High-Resolution Radar Rainfall Assimilation: Exploratory Studies with Latent Heat Nudging, 103pp, CHF 81.-

70 Müller G und Viatte P: 2005, The Swiss Contribution to the Global Atmosphere Watch Programme – Achievements of the First Decade and Future Prospects, 112pp, CHF 83.-

69 Müller WA: 2004, Analysis and Prediction of the European Winter Climate, 115pp, CHF 34.

68 Bader S: 2004, Das Schweizer Klima im Trend: Temperatur- und Niederschlagsentwicklung seit 1864, 48pp, CHF 18.-

67 Begert M, Seiz G, Schlegel T, Musa M, Baudraz G und Moesch M: 2003, Homogenisierung von Klimamessreihen der Schweiz und Bestimmung der Normwerte 1961-1990, Schlussbericht des Projektes NORM90, 170pp, CHF 40.-

66 Schär Christoph, Binder Peter, Richner Hans (Eds.): 2003, International Conference on Alpine Meteorology and MAP Meeting 2003, Extended Abstracts volumes A and B, 580pp, CHF 100.

65 Stübi R: 2002, SONDEX / OZEX campaigns of dual ozone sondes flights: Report on the data analysis, 78pp, CHF 27.-

64 Bolliger M: 2002, On the characteristics of heavy precipitation systems observed by Meteosat-6 during the MAP-SOP, 116pp, CHF 36.-

63 Favaro G, Jeannet P, Stübi R: 2002, Re-evaluation and trend analysis of the Payerne ozone sounding, 99pp, CHF 33.-

62 Bettems JM: 2001, EUCOS impact study using the limited-area non-hydrostatic NWP model in operational use at MeteoSwiss, 17pp, CHF 12.-

61 Richner H, et al.: 1999, Grundlagen aerologischer Messungen speziell mittels der Schweizer Sonde SRS 400, 140pp, CHF 42.-

60 Gisler O: 1999, Zu r Methodik einer Beschreibung der Entwicklung des linearen Trends der Lufttemperatur über der Schweiz im Zeitabschnitt von 1864 bis 1990, 125pp, CHF 36.-

59 Bettems J-M: 1999, The impact of hypothetical wind profiler networks on numerical weather prediction in the Alpine region, 65pp, CHF 25.-

58 Baudenbacher, M: 1997, Homogenisierung langer Klimareihen, dargelegt am Beispiel der Lufttemperatur, 181pp, CHF 50.-

57 Bosshard, W: 1996, Homogenisierung klimatologischer Zeitreihen, dargelegt am Beispiel der relativen Sonnenscheindauer, 136pp, CHF 38.-

Frühere Veröffentlichungen und Arbeitsberichte finden sich unter
www.meteoschweiz.ch » Forschung » Publikationen

MeteoSchweiz
Krähbühlstrasse 58
CH-8044 Zürich

T +41 44 256 91 11
www.meteoschweiz.ch

MeteoSchweiz
Flugwetterzentrale
CH-8060 Zürich-Flughafen

T +41 43 816 20 10
www.meteoswiss.ch

MeteoSvizzera
Via ai Monti 146
CH-6605 Locarno Monti

T +41 91 756 23 11
www.meteosvizzera.ch

MétéoSuisse
7bis, av. de la Paix
CH-1211 Genève 2

T +41 22 716 28 28
www.meteosuisse.ch

MétéoSuisse
Chemin de l'Aérologie
CH-1530 Payerne

T +41 26 662 62 11
www.meteosuisse.ch